Nano Today 38 (2021) 101135

Contents lists available at ScienceDirect

Nano Today

journal homepage: www.elsevier.com/locate/nanotoday

Review

Nanowire-enabled bioelectronics

Anqi Zhang[a,*], Jae-Hyun Lee[a,b], Charles M. Lieber[a,c]

[a] Department of Chemistry and Chemical Biology, Harvard University, Cambridge, MA 02138, USA
[b] Center for Nanomedicine, Institute for Basic Science (IBS), Advanced Science Institute, Yonsei University, Seoul 03722, South Korea
[c] John A. Paulson School of Engineering and Applied Sciences, Harvard University, Cambridge, MA 02138, USA

ARTICLE INFO

Article history:
Received 15 September 2020
Received in revised form 9 February 2021
Accepted 13 March 2021
Available online 20 March 2021

Keywords:
Nanowire
Bioelectronics
Biosensor
Electrophysiology
Brain mapping

ABSTRACT

Bioelectronics explores the use of electronic devices for applications in signal transduction at their interfaces with biological systems. The miniaturization of the bioelectronic systems has enabled seamless integration at these interfaces and is providing new scientific and technological opportunities. In particular, nanowire-based devices can yield smaller sized and unique geometry detectors that are difficult to access with standard techniques, and thereby can provide advantages in sensitivity with reduced invasiveness. In this review, we focus on nanowire-enabled bioelectronics. First, we provide an overview of synthetic studies for designed growth of semiconductor nanowires of which structure and composition are controlled to enable key elements for bioelectronic devices. Second, we review nanowire field-effect transistor sensors for highly sensitive detection of biomolecules, their applications in diagnosis and drug discovery, and methods for sensitivity enhancement. We then turn to recent progress in nanowire-enabled studies of electrogenic cells, including cardiomyocytes and neurons. Representative advances in electrical recording using nanowire electronic devices for single cell measurements, cell network mapping, and three-dimensional recordings of synthetic and natural tissues, and in vivo brain mapping are highlighted. Finally, we overview the key challenges and opportunities of nanowires for fundamental research and translational applications.

Contents

* Corresponding author. Present address: Department of Chemical Engineering and Department of Bioengineering, Stanford University, Stanford, CA 94305, USA.
E-mail address: aqzhang@stanford.edu (A. Zhang).

https://doi.org/10.1016/j.nantod.2021.101135
1748-0132/

Introduction

Ever since Luigi Galvani discovered 'animal electricity' in 1780s [1], electronic devices have made significant contributions to biology and healthcare. The communication of electronic elements with biomolecules, cells and/or tissues is now defined as 'bioelectronics' with major research activities focused on many areas, including biosensors that can transduce biomolecule recognition events into electronic signals, and implantable devices that can monitor and modulate electrical signals in tissues [2,3]. Bioelectronic devices are also widely used in healthcare from blood glucose sensors that can monitor blood sugar levels of diabetes [4] to cardiac pacemakers [5] that help control abnormal heart rhythms.

Despite these healthcare successes, existing bioelectronic devices and tools remain limited in terms of sensitivity, spatial resolution, and biocompatibility, mostly due to mismatches in size and mechanical properties with the biological elements being detected. For example, the basic elements central to neuronal communication and signal propagation (e.g., synapses and ion channels) show that the biological length scale relevant to intercellular communication is on the nanometer scale. In this regard, nano-electronic devices represent the biological scale for building effective interfaces to communicate between cells, and thus could serve as the building units for a seamless interface of electronics with biological systems [2,3]. For many in-vivo tools and wearable/implantable healthcare applications, conventional devices are significantly more rigid than natural tissue, this mechanical mismatch has resulted in relative shear motion at the tissue-electronics interfaces, leading to deterioration of the recording and stimulation capabilities over time. In this regard, electronic tools that match structural, mechanical, biochemical and other key properties with the natural tissue could thus provide chronically-stable and seamless integration, and open up many new scientific and technological opportunities [6,7].

In this review, we focus extensively on inorganic nanowire (NW) bioelectronics, which have provided unique advantages for developing tools and devices with enhanced or new capabilities for both fundamental science and healthcare. The diameters of NWs are comparable to the size scale of many biological species, including proteins, nucleic acids and cellular structures. Thus, NWs configured as field effect transistors (FETs) have been used as sensitive real-time electricity-based detectors of biological species and cell membrane potentials, where the signal amplitude does not depend significantly on probe size and resistance [3,8]. In this regard, the carbon-based nano-bioelectronics, including carbon nanotube [9], graphene [10,11], and organic [12,13] devices, have also shown promise as bioelectronics (see Table 1 for a summary of the typical electrical properties of nanomaterial transistor biosensors). Compared to these other materials, a unique advantage of inorganic NW devices stems from the possibility of designing and preparing complex NWs with structure, composition, and doping profiles controlled from the atomic scale [14–16]. One example is the synthesis of kinked or U-shaped NWs with point-like FET detectors at their tips, which has further enabled bioprobes capable of intracellular recordings in a minimally-invasive manner [17]. Taking advantage of standard top-down fabrication approaches, vertical NW electrode arrays have been developed as a scalable intracellular recording platform of electrogenic cells [18–20]. Last, arrays of NWs devices assembled and integrated on ultra-flexible, macroporous and biocompatible polymer mesh electronics have opened up measurements of cellular activity within synthetic and natural tissues [21–23]. In comparison, carbon nanotubes are synthesized as a mixture of semiconducting and metallic tubes. Such mixtures require purification for high-performance (semiconductor) devices, which may be challenging for scalable implementation [3]. 2D graphene-based devices, on the other hand, are more suitable for lower-resolution tissue-level interfacing, as their planar configuration can make difficult the formation of a tight seal with the cell membrane and significantly limits the signal amplitude [24]. Synthetic and natural polymer-based devices integrated onto flexible and stretchable substrates have shown good biocompatibility and reduced mechanical mismatch at the tissue-electronics interfaces, but their applications as nano-bioelectronics are still limited by the lack of synthetic control and patterning approaches at the nanometer scale [12,13].

Nanowire materials

The basic NW has a uniform 1D structure with diameters typically from 3 to 500 nm and lengths from several hundreds of nanometers to millimeters [14–16,25]. The first work in this area [26] showed that the vapor–liquid–solid (VLS) growth mechanism could be used to grow silicon (Si) and germanium (Ge) NWs where a metal nanocluster catalyst is used to direct the material growth along one direction. In the growth process, the metal nanocluster catalyst forms a liquid metal–semiconductor eutectic alloy by absorbing vapor phase reactant of the desired NW product, and when supersaturated, the nanocluster undergoes a nucleation event to form a crystallite of the semiconductor material. Continued absorption of reactant with the temperature above the liquidus temperature results in rapid elongation of the NW with the diameter defined approximately by the nanocluster catalyst (Fig. 1, top). The nanocluster-catalyzed VLS method has subsequently been extended to the growth of a broad range of NW materials, including group III–V (e.g., GaAs, GaP, GaN, InAs, InP, InSb) and II–VI compound materials (e.g., ZnS, ZnSe, CdS, CdSe) [16,27].

In addition, controlling dopant incorporation in NWs during growth is critical for making functional electronic devices [28]. For example, p- and n-type doping in Si and Ge NWs can be achieved by introducing gas precursors such as diborane and phosphine, respectively, where dopants may enter in the axial direction via the metal catalyst particle and liquid/solid interface or via radial

Table 1
Typical properties of nanomaterial transistor biosensors.

	SiNWs	Carbon nanotubes	Graphene
Transconductance ($\mu S\ V^{-1}$)	0.5–5 [179]	0.5–1 [212]	100–500 [213]
Mobility ($cm^2\ V^{-1}\ s^{-1}$)	100–1500 [68]	2000–100,000 [214,215]	3000–200,000 [216]
Gate capacitance	0.2–0.5 nF/m [217]	~ 0.4 nF/m [218]	~ 10 $\mu F/cm^2$ [219]
Limit of detection (mol/L)[a]	3.3×10^{-17} [83,220]	9×10^{-15} [221]	1×10^{-15} [222]

[a] Lowest limit of detection reported for prostate cancer biomarkers in buffer solution.

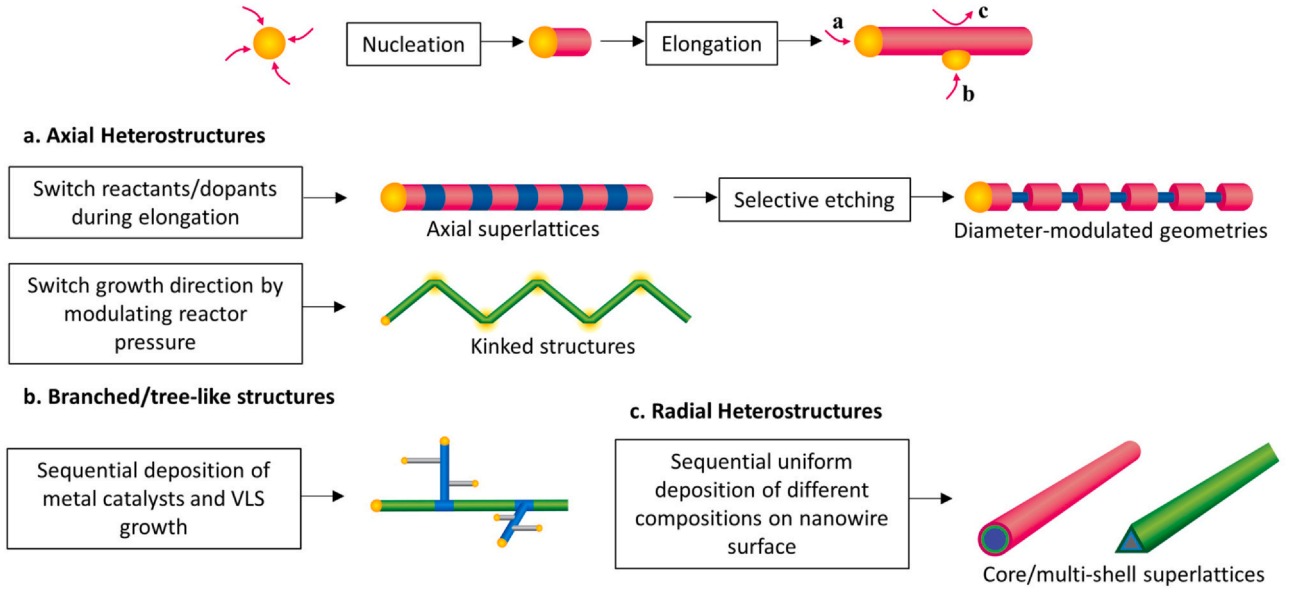

Fig. 1. Structure-controlled synthesis of nanowires. Top, schematic illustration of VLS growth of NWs. Vapor phase reactants undergo nucleation and growth of crystals in the presence of metal nanoparticle catalyst. a, Axial heterostructures. Switching dopants and/or modulating reactor pressure during NW growth enables control of NW structure in the axial direction. b, Branched/tree-like structures. Sequential deposition of metal catalysts on synthesized NWs enables branched and tree-like heterostructures. c, Radial heterostructures. Uniform layer-by-layer deposition on NWs enables control of NW structure in the radial direction.

deposition. Quantitative measurements of radial distribution of dopants has contributed substantially to understanding of device behavior [29]. The gate capacitance of boron-doped SiNW transistors has revealed non-uniform radial dopant profiles with higher dopant concentrations at the surface [30]. Atom probe tomography has been used to further show that differences in precursor decomposition rates between the liquid catalyst and solid NW surface can give rise to a heavily doped shell surrounding an underdoped core [31]. Consistent with these results, the dopant location assessed by electrical transport measurements with controlled removal of material from NW surfaces showed a well-defined transition from bulk-like to surface doping states as the NW diameter is decreased < 22–25 nm [32]. More uniform radial dopant profiles have been achieved by reducing dopant absorption on the radial NW surfaces and post-growth thermal annealing [33], as well as elevating the growth temperature [34].

The basic nanocluster-catalyzed VLS method for NW synthesis has been expanded significantly to controlled growth of NWs with modulated morphologies and structures, including axial heterostructures, branched/tree-like structures, and radial heterostructures (Fig. 1), where the increased complexity in the NWs offers unique functional advantages in the field of bioelectronics. Early studies of NW heterostructures [35,36] demonstrated the synthesis of axially modulated heterostructures by switching between different vapor phase reactants/dopants during NW elongation (Fig. 1a). Similarly, switching between different dopant concentrations and/or types has been used to produce dopant modulated heterostructures [37,38]. The combination of doping modulation and selective wet-chemical etching has been demonstrated to form synthetically encoded 10-nm resolution diameter-modulated geometries along the NW growth axis [39]. Pressure-dependent formation of Au-atom patterns in NWs (from the Au-nanoparticle catalyst) have been used to yield periodic axial structures after wet-chemical etching, where gold serves as an etch stop [40,41]. In addition, Plateau–Rayleigh-type NW growth has been achieved, mimicking stream of fluid breaking into smaller packets, to demonstrate tunable features on NWs such as periodic diameter modulation and anisotropic cross sections [42]. These periodic axial structures have the potential for helping to form tighter seals with tissues or other soft biomaterials [40].

The VLS growth mechanism can be further extended to the synthesis of kinked NWs produced by perturbation during NW growth, such as modulation of the reactor pressure [43], NW diameter [44], and electrical field [45] (Fig. 1a). For example, studies have suggested that cycles of reducing and increasing the NW reactants to stop and to restart nucleation and elongation will result in 1-kink/cycle as a result of re-nucleation occurring to minimize energy, and thus switching NW growth direction [43,46]. This technique can be combined with in situ doping modulation by introducing different dopant precursors during NW growth, yielding p–n junctions or transistors [17,43] synthetically encoded at the tips of kinks, which has enabled three dimensional probes capable of intracellular recordings in a minimally-invasive manner [17]. Alternatively, kinked NWs can be synthesized by 'welding' two crossed NWs to create heterostructure junctions with unlimited angle and potentially any composition and doping [47].

Control of junction sharpness in axial NW heterostructures is important to device function, and can be controlled with gradual to atomically abrupt interfaces that can synthetically define nanoscale sensing elements for interfacing with biomolecules or cells. Gradual transitions on the order of the NW diameter are due to a reservoir effect, i.e., slow depletion and re-equilibration of the liquid alloy catalyst with new materials [48]. To increase junction abruptness, several approaches have been demonstrated. A catalyst alloy, such as Ga–Au, that has a lower solubility of the target NW material can improve junction abruptness to ca. 0.2× diameter [49]. Alternatively, reduction of the growth temperature below the liquid solution point enables vapor–solid–solid (VSS) mechanism, where the low solid solubility of NW precursor has enabled the growth of atomically abrupt interfaces in Si/Ge and Si dopant-modulated NW heterostructures [50]. Related to these methods, sharp interfaces in In-As–GaAs heterostructures can be achieved by purging the reactant of Ga (or In) before the next segment is grown [51], or in the case of III–V–V heterostructures, taking advantage of the very low group-V solubility in the Au–III alloy catalyst to achieve atomically-abrupt NW junctions [29,36,52]. The sharp heterostructure interfaces has been utilized to achieve ultrashort-channel NW transistors for point-like cellular signal detection and potentially ion channel activity measurement on the length scale of single ion channels [50].

Branched or tree-like NWs can be obtained by introducing new nanocluster catalysts onto the primary NW 'trunk' (Fig. 1b) followed by VLS growth of the 'branches'. Repetitive nanocluster deposition and growth cycles then leads to hyperbranched NW structures, where each generation of NW branches can have a unique diameter and composition [53–55]. The branches on the NW trunk could be used as an 'antenna' to capture analytes for NW biosensors [56] or an ultra-sharp probe that can be inserted into electrogenic cells for intracellular electrophysiological recording [57]. Radial NW heterostructures can be rationally-prepared by sequential deposition of shells on the surface of a NW core to create core/shell or core/multi-shell structures [58,59] (Fig. 1c). One application of radial NW heterostructures in bioelectronics demonstrated the use of coaxial p-type/intrinsic/n-type SiNWs for modulating neuron excitability [60].

Nanowire-enabled biosensors

Basics of nanowire biosensors

The mechanism underlying NW FET biosensors is that the conductance at constant source–drain bias voltage will change in response to the binding of chemical and biological species at the NW surface, in a way similar to applying an external electric potential to gate electrode in a conventional FET device. For instance, in a p-type NW, binding of molecules with negative charges, similar to applying a negative gate voltage, leads to a corresponding increase in conductance. Specific detection is achieved by modifying the NW surface with receptor molecules selective to a specific chemical or biological species (Fig. 2a). A detailed mechanism, sensitivity and signal resolution of NW FET biosensors are summarized in Box 1.

SiNWs are a widely studied NW material for FET biosensors with advantages, including (i) controlled variation of n- and p-type dopants, (ii) capability to exploit well-developed surface chemistry to functionalize the surface silicon oxide layer, and (iii) potential of interfacing with standard silicon technology [3]. For SiNWs, a thin native oxide layer forms on the surface upon exposure to the air, which serves as a convenient substrate to conjugate functional groups (e.g., amine, thiol and aldehyde groups) with subsequent covalent immobilization via silane chemistry [64]. The amine modified surface of NW is routinely used for modification with antigen-targeting molecules, such as antibodies, that allow the NW FETs to achieve selective detection.

The earliest established example of this concept demonstrated pH and protein sensing [64]. In the case of pH sensing, NWs were functionalized using amino-silane molecules, where the surface charge state changes in response to hydrogen ion concentration from pH 2 to 9 [64]. SiNW FETs passivated with lipid bilayers containing ligand- and voltage-gated ion channels or proton-permeable carbon nanotube channels were employed to monitor the solution pH [65,66]. As an example of protein detection, SiNWs functionalized with biotin were used to detect streptavidin selectively at concentrations as low as 10 picomolar, although the strong and irreversible biotin–streptavidin interaction precluded monitoring unbinding of streptavidin [64]. Extending this concept to reversible protein binding interactions has allowed silicon and other NW FETs to demonstrate quantitative concentration-dependent monitoring and selective detection of a wide range of proteins [61,64,67–69] and sequence-specific nucleic acids [70–74] down to the femtomolar level, as well as even single-virus [75,76] and single-protein [77] detection.

A typical reversible binding cycle for NW FET measurements consists of association and dissociation phases (Fig. 2b) where time scale and analyte concentration define the association and dissociation rate constants. Significantly, SiNW FETs have been used to determine the kinetics of protein–receptor binding pairs with both slow and fast association/dissociation rates [78], a capability useful for screening protein interactions. Similarly, real-time NW sensing measurements have also been utilized to extract DNA-hybridization kinetic parameters [72]. This association/dissociation rate constants can in turn be used to distinguish specific binding from nonspecific adsorption as the specific binding shows faster kinetics than non-specific adsorption. For example, the sensing curves of SiNW FETs functionalized by antibodies against TROY, a tumor necrosis factor receptor, were compared with those of bovine serum albumin (BSA) as the nonspecific adsorption control [79], which exhibits significantly longer times scales to reach the similar signal amplitudes as to that of TROY.

Typically, the sensor response is measured after the value reaches a steady state. For ultralow-concentration detection where the analyte transport process becomes the limiting step, the duration of the association phase is greatly extended and might require tens of minutes or even hours to perform one sensing task. Potential methods for circumventing such long measurement times include: i) selecting high binding affinity receptors that make contributions from the minimal unbinding rate, ii) modulating the charge state of the analytes to accelerate drift transport to the NW surface and iii) locally defining the surface functionalization only on the NW surface instead of the entire chip area to suppress competitive binding and further analyte depletion due to substrate binding [80].

Potential for disease detection and treatment

Simultaneous detection of multiple proteins is especially important for diagnosing complex diseases, and different biomarkers matched with different stages of diseases could allow for early diagnosis [81]. In 2005, integrated NW sensor arrays was developed [61], in which ~ 100 individually addressable NW FETs were functionalized with different biomarker receptors (Fig. 2c, left) enabling parallel detection of the cancer marker proteins such as prostate specific antigen (PSA), carcinoembryonic antigen (CEA), and mucin-1. Conductance measurements recorded simultaneously from three such NWs showed signals with femtomolar sensitivity (Fig. 2c, right). In 2012, parallel detection of the cardiac biomarkers [82], troponin-T, creatine kinase MM, and creatine kinase MB, was achieved with femtomolar sensitivity in serum using an antibody-functionalized SiNW biosensor arrays. In another report, a two-channel microfluidic system integrated with SiNW FET arrays was used for ultrasensitive detection for two cancer biomarkers, cytokeratin 19 fragment (CYFRA21-1) and PSA, in both buffer solution and undiluted human serums [83]. The parallel sensing capability has been extended to simultaneous detection of different species, such as the lung cancer biomarkers miRNA-126 and CEA [84]. Further increases in the scalability and decrease in sensor-to-sensor variations promise to bring NW sensor technology a step closer to commercial products for early diagnosis and monitoring of diseases [85].

The potential of NW arrays as cancer diagnostic tools has also been demonstrated by the detection of the activity of telomerase, which is widely expressed in most human cancers but is inactive in most normal somatic cells. The presence of the positively charged telomerase was readily monitored by p-type NWs as a conductance decrease, where the NW arrays are modified with the telomeric repeat sequence. Subsequent addition of deoxynucleotide triphosphates (dNTPs) further allowed for monitoring of telomerase activity through conductance increases due to the incorporation of negatively charged nucleotides near the NW surface [61] (Fig. 2d). The inhibition of telomerase elongation activity has also been investigated by adding a reverse transcriptase inhibitor (Fig. 2d, lower right) [61], together demonstrating the sensitivity and selectivity of NW sensors for telomerase detection and activity, potentially applicable in cancer cell assays as well as screening of potential inhibitors.

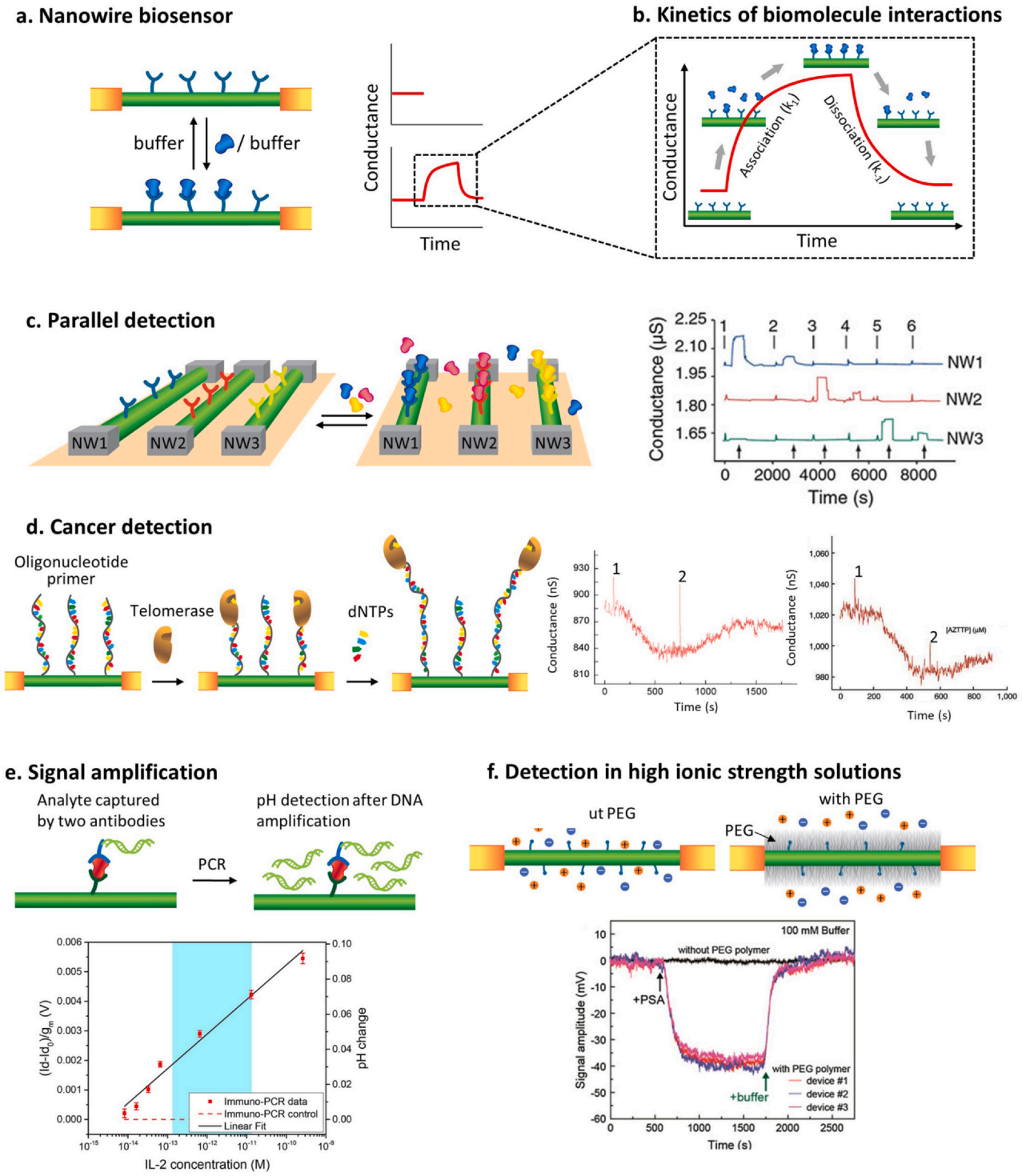

Fig. 2. Nanowire biosensors. a, A NW FET biosensor for specific detection. Binding of charged analytes yields a change in the NW conductance. b, Conductance changes during association and dissociation phases of biomolecules on NWs. c, Parallel detection. Left, parallel detection by NW devices modified with different protein receptors. Right, conductance vs. time data for simultaneous detection of different proteins. d, Cancer detection. Left, telomerase detection and incorporation of activated nucleotides, dNTPs. Middle, conductance vs. time data for telomerase detection (point 1), and subsequent addition of dNTPs (point 2). Right, conductance vs. time data for telomerase detection (point 1) and inhibition of telomerase elongation (point 2). e, Signal amplification. Top, biomarker detection with the help of exponential DNA amplification with polymerase chain reaction (PCR) process. The protein sensing is translated to pH measurement by NW FET sensors. Bottom, pH sensing response by NW FETs vs. IL-2 biomarker concentration with immuno-PCR on NWs. f, Detection in high ionic strength solutions. Top, PEG surface modification on NW devices. Bottom, conductance vs. time data from devices with and without PEG modification in high ionic strength solutions.
Panel c and d are adapted with permission from Ref. [61], Macmillan Publishers Limited. Panel e is adapted with permission from Ref. [62], American Chemical Society. Panel f is adapted with permission from Ref. [63], American Chemical Society.

In addition to cancer biomarkers, the detection of disseminated tumor cells in cancer patient lymph nodes is also an important prognostic indicator in many types of cancer [86]. Using keratin antigen as the marker of tumor-derived epithelial cells, SiNW FETs could detect the presence of a single tumor cell from the lysate of a whole lymph node. Furthermore, a small number of circulating

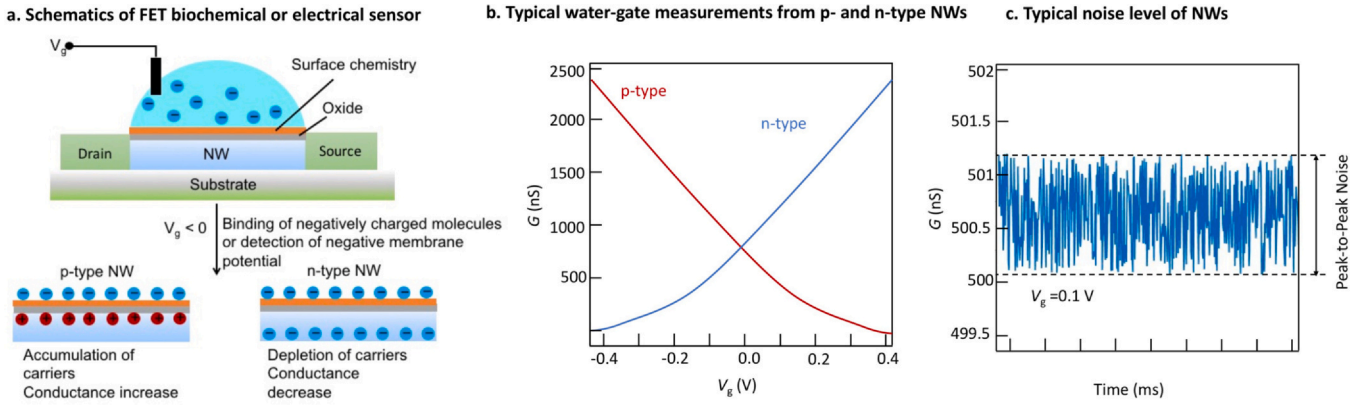

Box 1. Nanowire transistor sensors: sensitivity and signal detection. In a field-effect transistor (FET), the semiconductor material is connected to source (S) and drain (D) electrodes, which are used to inject and collect current, respectively. The conductance, G, is given by dI_{ds}/dV_{ds}, where I_{ds} and V_{ds} refer to source–drain current and bias voltage, respectively. A third electrode, the gate (G) electrode, which is capacitively coupled to the semiconductor channel by an insulating oxide layer, modulates the conductance between the source and drain electrodes [109]. The basic electronic properties of a NW sensor can be characterized in the FET configuration. G can be modulated by variations in the electric field at the NW FET surface resulting from binding of charged molecules or changes in cell membrane potential, analogous to varying the gate voltage in a solid-state FET (panel a). Characterization of individual NW FET devices in aqueous solution is performed by measuring G as a function of the water-gate potential, V_g, while applying a fixed V_{ds} (panel b). The slope extrapolated from the linear region of the G–V_g plot is defined as sensitivity or transconductance $g_m = dG/dV_g$ [109], which is typically on the scale of several microsiemens per volt [179]. Thus, the measured conductance change, ΔG, can be converted to an absolute voltage signal V_g using g_m [63,134]. In addition, the resolvable signal in the linear response regime is ultimately defined by the noise level under the measurement conditions (e.g., panel c) [21,134]. In high ionic strength solutions, the charges of bound analytes can be screened by solution counter ions. This effect, referred to as the Debye screening effect [99,112], affects the signal amplitude of NW FET biochemical sensors. The Debye length λ_D is defined as $\lambda_D = \sqrt{\frac{\varepsilon_0 \varepsilon_r k_B T}{2N_A e^2 I}}$, where ε_0 corresponds to the vacuum permittivity, ε_r is the relative permittivity of the medium, k_B is the Boltzmann constant, T is the temperature, N_A is the Avogadro number, e is the charge of an electron, and I is the ionic strength of the solution. A high ionic strength electrolyte solution leads to a short Debye length, and charges outside of the Debye length are electrically screened, and thus cannot affect G.

tumor cells (1–10 cells per 10^6 leukocytes) are released by tumors in peripheral blood early in their formation. The keratin-targeting SiNW FET platform was utilized for monitoring cancer metastasis, by the detection of circulating tumor cells in colorectal cancer patient's blood, with a detection limitation of as low as 2.5 cells/mL of blood [87].

One alternative approach for cancer detection is based on volatile organic compounds (VOCs) produced by the cancer cells. At very early stages of cancer, VOCs are generated by cellular metabolic pathways during blood circulation and diffuse into exhaled breath, their isolation and detection could thus serve as a noninvasive pathway for early detection and prognostic monitoring of the cancer [88]. Specifically, molecularly modified SiNW FETs have enabled the detection and classification of several disease breathprints from lung cancer, gastric cancer, asthma, and chronic obstructive pulmonary disease patients, with a VOC detection limit at low parts-per-billion concentrations [89,90]. Combined with pattern-recognition methods and machine learning, these sensors were able to recognize complex mixtures of VOCs and discriminate between cancer patients and healthy individuals with > 85% accuracy, irrespective of confounding factors such as tobacco consumption and gender.

Identification of small molecules that bind specifically to proteins is central to the discovery and development of new pharmaceuticals and to elucidating pathways in biological systems. Specific to discovery of drugs to treat disease is the identification of molecular inhibitors of tyrosine kinases, which are central elements in signal transduction networks. The regulatory function of tyrosine kinases occurs through phosphorylation of a tyrosine residue of a substrate protein using adenosine triphosphate (ATP) [91]. To screen tyrosine kinase inhibitors, NW sensors modified with the Ab1 tyrosine kinase have been used to investigate the binding of ATP and the inhibition of ATP binding with organic molecules, such as the drug Gleevec [92]. In addition to Gleevec, which is a known tyrosine kinase inhibitor, measurements of competitive inhibition of ATP binding by three small molecules (A1, A2 and A3) using Ab1-modified NW devices showed structure-dependent inhibition in order Gleevec > A1 > A2 > A3 ≫ control [92], thus further highlighting the potential of NWs as a nanotechnology platform for drug discovery and screening.

Sensitivity enhancement

Intrinsic nanowire biosensor properties

The sensitivity of NW FETs is critically dependent on the size of NWs [93]. The sensing sensitivity of NW sensors has been proved to be much higher than microwire devices. The increased sensitivity for smaller sizes is attributed to the larger surface/volume ratio for smaller wires exposing a larger volume percentage of the channel to control by the local environment. Along this line, creating nanoscale patterns on NW surface could also increase the surface area and thus enhance sensitivity [94,95]. In addition, lower NW doping densities results in higher device sensitivity, which may be attributed to the reduced effect of charge screening by mobile charge carriers in NWs [96]. For SiNW biosensors, the native oxide on the NW surface serves as the gate oxide. Outside of thicker gate oxide, the electric field generated by the charged analytes present smaller influence on the conductance of the channel. Therefore, the sensitivity increases with decreasing oxide thickness [97]. Furthermore, device sensitivity decreases with increasing number of NWs per channel [98]. For a multi-NW FET device in which several closely spaced NWs compete for the binding of free analyte molecules, the number of NW-analyte interactions per NW is expected to decrease as the number of NWs increases, resulting in a smaller response from each NW.

Selective surface modification

The surface of NW devices has been modified to enhance the selectivity and specificity for antigens. As discussed previously, the functionalization of NW surfaces starts with silane chemistry and followed by receptor modification to form covalent bonding. This modification step is non-selective, i.e., receptor molecules will be conjugated on both NWs and the surrounding substrate (typically with an oxide surface, such as silicon wafers and glasses). Thus, the probability of analyte molecules coming in contact with the NW surface is very low, especially for highly diluted analyte solutions. Several approaches of selective surface modification [99–104] have been developed, to modify only the NW surface. For example, an electrical bias was applied on the SiNWs to create a localized heating

effect at the low doping sensing region, where the surface conjugation reactions can be locally initiated [100,103].

In addition, the quality of the surface coating is important for achieving reproducible and highly sensitive detection [105,106]. For example, structural ordering of the surface-modified monolayer can be crucial for high sensitivity since a well-aligned molecular monolayer can collectively enhance charge polarization induced by molecular interactions. One approach to achieving homogeneous monolayer was to align surface molecules to an externally applied electrical field [105], which has yielded a significant enhancement of the detection sensitivity and reliability for DNA and alcohol sensors. Notably, another report suggested that the orientation of antibodies can greatly influence the sensing efficiency [107], since the randomly oriented receptors have only a fraction of them with the binding site exposed correctly to bind with their antigens. This problem was partially solved by aligning antibodies with an external electric field. For two different CEA-related cell adhesion molecules 5 (CEACAM5) & 1 (CEACAM1) detected with antibody-modified NW sensors, atomic force microscopy found that antibodies with optimal angles have the binding force reached its maximum where the signal becomes more stable.

Signal amplification

In some cases where the direct sensing responses are too small, signal transduction approached have been developed, where the weak signal events can be translated to strong signal events. One example for improving DNA detection sensitivity utilizes a DNA amplification technique called rolling circle amplification (RCA) [108]. The capture probe DNA was conjugated to SiNWs and hybridized with fully matched target DNA and another DNA sequence called RCA primer. Subsequently, DNA amplification reaction was carried out at the location of the RCA primer, which led to significantly enhanced signal recorded by the NWs, compared to direct DNA detection.

Another example involves disease marker detection in serum with the help of exponential DNA amplification, where the protein sensing is translated to pH measurement by NW FET sensors (Fig. 2e) [62]. The antigens interleukin-2 (IL-2), the marker for immune response, were first captured by two antibodies with the sandwich-type assay, one of which immobilized on a substrate, and the other labeled by a DNA strand. The DNA strands were then exponentially amplified by polymerase chain reaction (PCR). The attachment of each nucleotide to the nucleic acid strand resulted in the release of a proton, changing the pH of the solution, which can then be detected by NW FETs, and used to quantify the antigens in the original serum samples, while the control group without DNA amplification showed no detectable response. The detectable concentration of interleukin-2 ranges from ca. 20 fM to 200 pM. The use of two antibodies can effectively decrease the nonspecific adsorption, and the pH measurement is immune to the limitations of direct protein sensing. Further improvement of this work can be made by incorporating PCR elements into the sensing setup and achieve real-time detection.

Detection in the subthreshold regime

Typically, NW FET sensors are operated above the threshold voltage, where the transconductance depends linearly on gate-voltage. However, in the subthreshold regime, the device conductance depends exponentially on gate voltage [109], which could in principle lead to much higher analyte binding sensitivity. Indeed, the detection sensitivity of SiNW FET sensors operating in the subthreshold regime was significantly enhanced by ~ 500 times compared to those operating in the linear regime [94,110,111], suggesting that sensitivity enhancement can be achieved by optimization of the FET operating conditions and understanding the fundamental electrical gating property of NW FETs. One caveat to the success subthreshold detection is that the device noise should be dominated by carrier–carrier scattering, such that the noise is also exponentially reduced in the subthreshold regime. If the noise is dominated by other scattering mechanisms, such as contact current injection and/or interface trapping/detrapping, then it may not be possible to exploit the exponential dependence of conductance on gate voltage/surface potential in the subthreshold regime.

Towards point-of-care detection

FET sensors detect the concentration of the target species by their intrinsic charge, however, these charges can be screened by counter ions in physiological solutions. The Debye length, which is inversely proportional to the square root of the ionic strength of an electrolyte, represents the screened electrostatic effect of charged species in ionic solution (Box 1). A high ionic strength electrolyte solution leads to a short Debye length, and charges outside of the Debye length are electrically screened. For instance, the Debye length of high ionic strength physiological solutions (i.e., 100 mM), < 1 nm, can screen most protein antigen charges when they bind to an antibody-modified FET surface [112].

One commonly used method for detection in high ionic strength solutions involves an initial 'desalting' step prior to NW FET detection [61,113,114]. For example, the use of a microfluidic chip was reported that can simultaneously capture multiple biomarkers from whole blood samples and release them into low-ionic strength buffer for sensing by SiNWs [113]. Other reported approaches for high-ionic strength detection have focused on smaller receptors, such as aptamers [115–117] and antibody fragments [118], to reduce the distance between the FET surface and biomolecule analytes. Additionally, conformational changes of highly charged aptamers upon protein binding can result in a significant change in electric field near the sensor surface, thereby enabling highly sensitive detection of both charged and electroneutral molecules [119,120]. Another strategy is based on high-frequency measurements, where an alternating current field was applied to disrupt the electrical double layer (EDL), leading to deeper penetration of the electric potential of the target biomolecule, and therefore increasing the NW response to the fluctuating dipoles of the target molecule [121,122], although the more complex device geometry makes applications to cellular or in vivo sensing more challenging.

Another general strategy developed to overcome this challenge for FET sensors involves incorporating a biomolecule-permeable polyethylene glycol (PEG) polymer layer on the FET sensor, where the polymer increases the effective screening length near the NW FET surface to allow for detection in high ionic strength solutions (Fig. 2f) [63]. PEG-modified devices were able to detect PSA directly at physiological ionic strengths. The effect of increased Debye length of the confined ions inside the polymer layer has been confirmed [123]. In addition, the PEG layer could contribute to enhanced sensitivity and selectivity in complex physiological environments due to its nonspecific adhesion suppressing capacity; conjugating antibodies on NWs using a PEG cross-linker has also been proved to enhance biosensing efficiency by decreasing steric hindrance for antigen binding [124]. These studies suggest a general device design strategy for the FET sensor applications in physiological environments, which is important for in vitro and in vivo biological sensing.

Other works in this field have explored indirect approaches to circumvent the Debye screening limitation in high ionic strength physiological solutions [62,125]. For example, the application of antigen-dissociation regime was demonstrated as an effective sensing mechanism in untreated serum and blood samples [125]. Specifically, the biosamples were first introduced to antibody-modified NW FETs to allow the binding of antigens, after complete association of the target antigens, low ionic strength buffer was introduced to 'flush out' the NW FETs to sequentially remove the unbound biomolecules and specifically bound antigens in a manner that depends upon the strength of the interaction. The two-stage dissociation

curve measured by NWs, corresponding to the fast and slow dissociation steps, was extracted to calculate the antigen concentration. It is worth noting that the key to performing quantitative analysis is that the affinity strength of the antibody–antigen recognition pair which must be significantly higher than nonspecific binding of other proteins on antibodies. Ultimately, point-of-care diagnostics will require rapid analysis of clinically relevant samples such as blood, where a successful example is the personal glucose meter [4]. A small drop of blood is placed on a test strip, and the blood glucose concentration can be output using an electronic reader. Based on the studies discussed above, the concept of blood analysis can potentially be expanded to the detection of i) serum proteins and disease markers, ii) viruses and pathogens, and iii) genomic DNA sequence variations. The combination of parallel sensing, detection in physiological solutions and integration of NW sensor arrays into portable devices has the potential to revolutionize disease diagnosis and patient monitoring.

Nanowire probes for cellular activity

Monitoring cell electrophysiology

Electrophysiology is an important approach to investigate and understand the activity of electrogenic cells, such as neurons and cardiomyocytes. The glass micropipette-based electrode [126] is established as the standard for cell electrophysiology recording, although has limitations in terms of size needed to probe key subcellular elements such as synapses and ion channels, invasiveness and applicability to large-scale recording [3,8,18,20,127]. NW FETs, which can reach critical biological length scales, represent attractive candidates for next generation cell electrophysiology tools that enable parallel and long-term detection of both intracellular and extracellular activity with high spatial and temporal resolutions [3]. The underlying mechanisms by which devices can record electrophysiological changes due to ionic current flows across the cell membrane are highlighted in Box 2 and have been reviewed elsewhere [8,18,20,128].

Neurons transmit signals over long distances by propagating action potentials along their axons and dendrites. In 2006, NW FET arrays were first applied to extracellular recording of neuronal activity at the level of individual axons/dendrites [129]. Patterned growth of axons and dendrites over SiNW FET arrays yielded synapse-like junctions with highly-localized 0.01–0.02 μm^2 contacts, thus enabling multisite recording with multiple SiNW FET devices from single neurons, in contrast to the typical one neuron per electrode achieved with micropipette recording (Fig. 3a, top). Similar protruding nanostructures have been demonstrated to generate intimate membrane/nanostructure junctions than planar substrates [130–132] (Fig. 3a, lower left), which improves the seal resistance and thus the extracellular signal amplitude. Notably, the extracellular signal in this work resembles the intracellular action potentials, indicating the leak conductance dominates at the membrane/NW interface (Box 2) [133]. The potential of this approach was further shown by recording action potential propagation with 50 independently addressable NW–axon elements from a single neuron. These results showed the potential of NW FET sensors for enabling new capabilities of recording sub-cellular signals and now recognized as critical to brain science initiatives.

Cardiomyocytes represent another electrogenic cell type that have been extensively studied with bioelectronic devices [50,134–137]. Parallel measurements made with SiNW FET device arrays interfaced with cultured cardiomyocytes recorded action potential peaks of the beating cells [134]. Subsequent studies using SiNWs with axially encoded FET channel lengths of 50, 80, and 150 nm showed that the recorded action potential width was found to be comparable to the reported time constant for individual sodium ion channels, thus suggesting the possibility of single ion channel studies (Fig. 3a, lower middle) [50]. In addition, several groups [135–137] reported extracellular recording from cardiac cells using top-down fabricated SiNW devices. In these studies, the extracellular signals resemble the first derivative of the intracellular action potentials, indicating the capacitive current dominates at the membrane/NW interface (Box 2) [133]. Future studies exploiting the chemical sensing capability of NW FETs to detect neurotransmitters such as dopamine (Fig. 3a, lower right) [115,119,138,139] could further increase the power of these studies by allowing simultaneous voltage and biochemical signals to be recorded in real-time. The electrical signals could be decoupled based on the different time scales, since action potentials are on the scale of 1-millisecond, while the biochemical signals such as dopamine release are on the scale of tens of milliseconds from a single synapse to several seconds from a brain region containing many cells [140].

Extracellular recording has advantages for long-term parallel measurements, although it is limited in capability to record

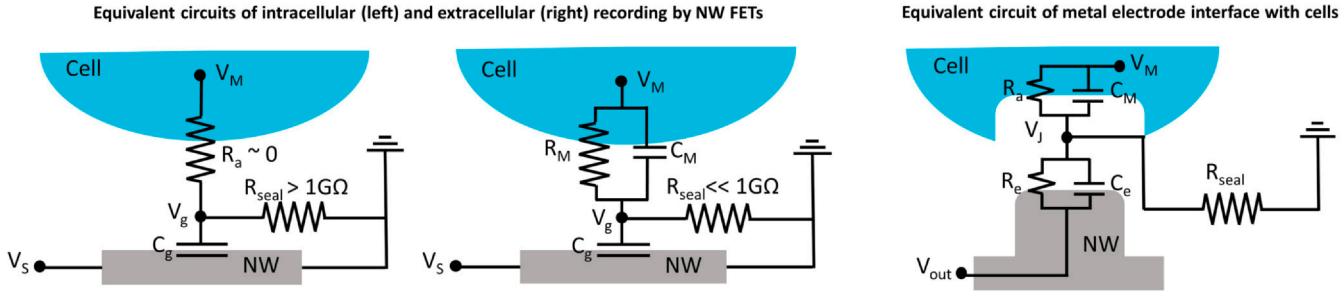

V_M: membrane potential; R_a: access resistance; V_g: gate voltage; R_{seal}: seal resistance; C_g: gate capacitance; V_S: source voltage; R_M: membrane resistance; C_M: membrane capacitance; V_J: junction voltage; R_e: electrode resistance; C_e: double layer capacitance; V_{out}: output voltage.

Box 2. Nanowire transistors and metal electrodes as electrogenic cell sensors. FET electrical sensors can be used for intracellular and extracellular electrophysiological recording from electrogenic cells (figure above), including neurons and cardiomyocytes. For intracellular recording, the access resistance R_a is negligible when the nanoscale sensing region is inserted into the cytosol, and surface functionalization of the electrodes using lipids contributes to the formation of GΩ resistance seals at the membrane/NW junction (R_{seal} > 1 GΩ). Under these conditions, full amplitude action potential signals (~ 80–100 mV) can be recorded. For extracellular recording, the cleft between the cell membrane and the FET surface determines R_{seal}, and the voltage drop over R_{seal} directly modulates the recorded signal. R_{seal} for micro- and nano-engineered junctions can approach or exceed 100 MΩ [8]. Two major models have been established for illustrating the possible shapes of the extracellular signals: [133] 1) when the leakage conductance of the attached membrane dominates, the signals retain the original action potential shape, but with smaller amplitude compared to true intracellular signals; and 2) when the capacitive current through the attached membrane dominates, the signals correspond to the first derivative of the intracellular action potential. The figure above shows the equivalent circuit of the interface between the metal electrode and the cell membrane. For intracellular recording, the access resistance R_a can be significantly reduced by membrane disruption methods such as electroporation [18]. The junction voltage V_J can be increased by reducing R_a and increasing R_{seal}. And the output voltage V_{out} can be increased by decreasing the electrode impedance, which can be achieved by using multiple NWs as a single electrode. We refer readers to other reviews [18,19,167] for more detailed analysis of this circuit model.

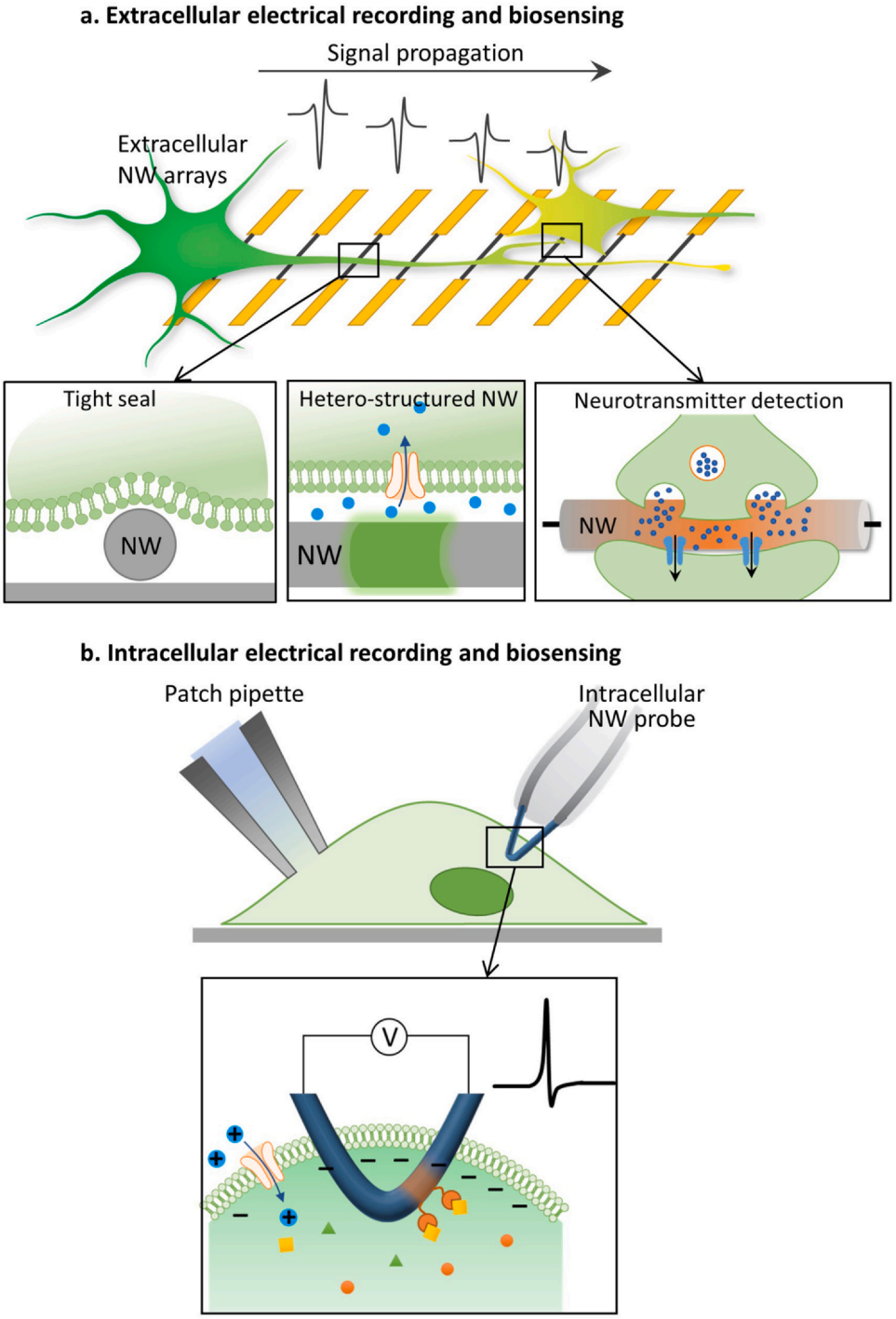

Fig. 3. Cell electrophysiology. a, Extracellular electrical recording and biosensing. Top, a neuronal axon aligned on an array of NW devices. Lower left, a tight seal formed between the NW and neuronal membrane. Lower middle, axial NW heterostructures with a sensing region on the same length scale with a single ion channel. Lower right, neurotransmitter detection at a neuronal synapse. b, Intracellular electrical recording and biosensing. Top, intracellular recording using a patch pipette and a kinked NW probe penetrating cell membrane. Bottom, biochemical sensing with FET NWs intracellularly penetrated through membrane for detecting and monitoring in situ kinetics of biomolecules in live cells.

subthreshold events important to circuit activity [8,127,141]. In addition, the ability to record extracellular voltage fluctuations is limited by the device noise in electrolytes and the seal resistance at the membrane/NW junction (Box 2). The stability of this seal determines the stability of long-term measurements. Intracellular recording using micropipette methods can record subthreshold signals, but are limited in terms of direct solution exchange with the cytosol and relatively large micron scale tip that could damage the membrane [3,8,18,20,127]. NWs are potentially ideal structures for intracellular probes because (i) their small size should allow for minimally-invasive insertion, (ii) as solid-state devices they will not leak into cells and (iii) NW FET devices can detect intracellular voltage nearly independent of interfacial impedance in contrast to passive electrode techniques. Despite these advantages, the size of the source and drain contacts of the conventional linear NW FETs precluded minimally-invasive insertion of a NW FETs into cells.

The first work [17] that overcame this electrical contact size constraint was achieved by the synthesis of nonlinear kinked NWs,

with a point-like FET synthetically encoded at the tip (Fig. 3b, top). Modification of the surfaces of the kinked-NW FET probes with phospholipid bilayers yielded spontaneous insertion through the cell membrane of beating cardiomyocytes and subsequent intracellular action potential was recorded with an average peak amplitude of ~ 80 mV and duration of ~ 200 ms as expected for these cells (see Box 2) [17]. Subsequent works developing NW tools for cellular recording include branched nanotube–NWs fabricated based on branched NW structures described in *Nanowire materials*, which showed intracellular action potential recording from cardiomyocytes where electrolyte in the intracellular nanotube gated the extracellular NW FET [57]. To provide deterministic control over probe–cell interactions, kinked NW FETs have also been fabricated on the tip of free-standing probes that can be manipulated in 3D to target specific subcellular regions [142]. Significantly, simultaneous NW FET and micropipette recording from the same beating cardiomyocytes showed the kinked NW probes recorded the same intracellular signals as the standard of electrophysiology, opening up new capabilities in terms of spatial resolution and biomimetic cellular targeting. The progress in intracellular recording described above has been made possible by the rational synthesis of complex semiconductor NW building blocks with nanoscale precision. The intracellular access achieved by NW probes can be further investigated to enable unique multi-functional bioprobes with the potential of sensing both intracellular electrical and chemical signals (Fig. 3b, bottom), in a way similar to what has been achieved using intracellular nanopipettes [143].

Vertical NW electrode arrays have recently been developed as a scalable intracellular recording platform of electrogenic cells [18–20]. These NWs typically have a height of a few micrometers, a diameter of tens to hundreds of nanometers. When cells are plated on top of NW arrays, the plasma membrane deforms and wraps around NWs, creating a tight seal at the interface [144,145]. In order to achieve intracellular access, the NWs need to come into direct contact with the cytosol [146]. Spontaneous perforation enabled intracellular recording has been reported [147,148], although the yield of spontaneous penetration of NWs into living cells has a low yield of only ~ 7% [149,150]. One recent work has shown that this yield may be increased by promoting tight adhesion and high local deformation of cell membrane in contact with NWs by increasing the edge sharpness [151]. On the other hand, controlled membrane disruption, such as electroporation [152–159], has been demonstrated to be a more reliable way of gaining intracellular access. Electroporation refers to the application of voltage/current pulses at the NW tips to transiently disrupt the local membrane patch. Typically, the action potential amplitude is significantly increased right after electroporation, and gradually reduces over time as membrane reseals. Another recent approach to achieving intracellular access in a more localized and less-invasive manner is plasmonic optoporation [160–163], where plasmonic NWs can be excited by short laser pulses to generate mechanical waves able to locally open transient nanopores in cell membrane. Alternatively, one approach that can avoid the use of physical triggers requires patterning nanoscale hydrophobic bands on otherwise hydrophilic nano-electrodes [164]. The lipid bilayer cell membranes are hydrophobic in nature, and upon insertion of the nano-electrode, the membranes fuse with the hydrophobic bands and form a stable interface. Inspired by this early demonstration, a recent study reported arrays of 3D ring-shaped electrodes fabricated in a layer-by-layer manner [165]. The middle layer, made of gold and functionalized with hydrophobic alkanethiols, protrudes from the structure to fuse with the cell membrane. As a result, these electrodes formed tight seal to the cultured neonatal rat cardiomyocytes, in a way similar to that of the patch pipettes. Signals recorded from up to 30% of the ring electrodes displayed the typical shape of intracellular action potentials.

In the recent studies of vertical NW array enabled intracellular recording, NW electrodes have been combined with complementary metal-oxide–semiconductor (CMOS) integrated circuits for parallel recordings at the network level [156,166]. The CMOS array has thousands of recording/stimulation sites, and can simultaneously record intracellular potentials from hundreds or thousands of connected in vitro cardiomyocytes and neurons. The NWs arrays are less invasive to cells than the traditional glass micropipette recording due to the lack of solution exchange at the interface. Compared to the bottom-up fabricated NW devices that require post-synthesis assembly, these top-down fabricated NW electrodes can be produced in a highly parallel manner to yield large-scale arrays. Such network-level intracellular recording capability can potentially be used for rapid sorting of cells according to their electrophysiology, as well as for monitoring and drug screening of cardiac and neuronal diseases [157]. Nevertheless, these studies also have limitations compared to NW FETs, including i) the signal-to-noise ratio depends on the electrochemical impedance of metal NWs (Box 2) [18,19,167], and ii) the signal amplitudes of intracellular potentials are still lower than those recorded by micropipettes. Additionally, the 2D substrate-based NW array platform is still not compatible with minimally invasive 3D in vivo recording.

The capability of NWs has also been extended recently to photoelectrochemical and photothermal stimulation. For example, coaxial p-type/intrinsic/n-type SiNWs have been demonstrated to directly modulate the excitability of primary rat dorsal root ganglion (DRG) neurons and cardiomyocytes [60,168,169]. Specifically, light stimulation of a coaxial SiNW at the NW/neuron interface generated electron movement to the n-type shell, which injects charge that can locally depolarize a target neuron and induce action potentials. In another work, SiNWs were dispersed onto a coculture of DRG neurons and glial cells, and were mainly internalized by the glial cells [170,171]. Laser illumination on the intracellular NWs induced a photothermal effect that resulted in a fast calcium wave in the targeted glial cell, which could propagate to neighboring glial cells and DRG neurons. The ability to achieve optically-controlled modulation of neuron activity without the need for genetic modification [172] can potentially be applied to both fundamental single-cell and subcellular studies and clinical therapeutics [173]. Recently, retinal neuron stimulation has also been achieved using photocurrent produced by NW arrays [174]. Specifically, titanium dioxide (TiO_2) NWs coated with Au nanoparticles were surgically introduced as subretinal implants to blind mice with degenerated photoreceptors. Upon exposure to green, blue and near UV light, TiO_2 NWs can produce a photocurrent that stimulates the neighboring retinal neurons as artificial photoreceptors, and thus restore the light sensitivity and visual function in the implanted eyes.

Monitoring cell metabolic activity

The NW FET biosensing platform has also been exploited for real-time localized monitoring of the activity of living cells [115,116,175,176]. For example, SiNW FETs modified with DNA aptamers selective for dopamine binding were able to detect dopamine release from Pheochromocytoma 12 (PC12) cells when the environmental O_2 concentration (C_{O2}) was decrease by 70%, although a less severe 35% C_{O2} reduction did not trigger release [115]. In addition, measurements carried out with Ca^{2+} channels blocked by Cd^{2+} ions showed no dopamine release under hypoxic stimulation.

The distinct and time-dependent concentration of simple ions, such as Na^+ and K^+, across the plasma membrane is an important physiological property of live cells. K^+ flux from live chromaffin cells was measured using SiNW FETs coated with a polyvinyl chloride (PVC) membrane containing valinomycin (VAL) [175], where VAL has a high affinity for K^+ relative to other alkali metal ions like Na^+. More recently, SiNW FETs modified with K^+-specific DNA aptamers have

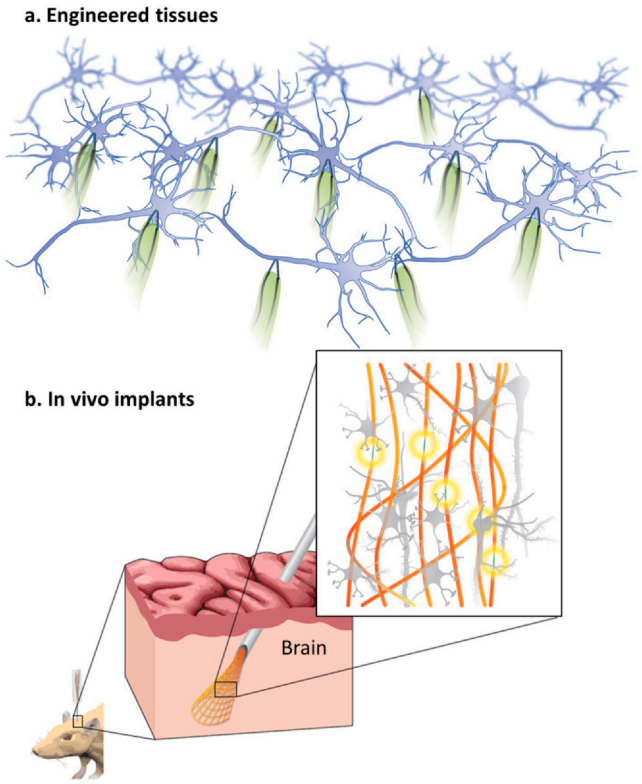

Fig. 4. Tissue electrophysiology. a, Engineered tissues. NW probe arrays interfaced with biological tissue could enable network-level parallel and scalable recording for extended time periods. b, In vivo implants. Ultra-flexible tissue-like electronics embedded with multiple NW devices can be injected into a rodent brain with a syringe needle. The highly porous structure allows seamless interpenetration with neural networks and enables chronic recording of brain activity.

been used for the real-time detection of the K^+ efflux from cultured cortical neurons [116] following α-amino-3-hydroxy-5-methyl-4-isoxazolepropionic acid (AMPA) stimulation. In another report, SiNW FETs have measured the extracellular Zn^{2+} concentration and revealed its effect on the fibrilization of amyloid-β (Aβ), a pathogenic factor for Alzheimer's disease. In glutamatergic neurons, the Zn^{2+} stored in the secretory vesicles is coreleased with glutamate upon stimulation, resulting in the elevation of extracellular Zn^{2+} concentration. The Zn^{2+} concentration was quantified in real time using SiNW FETs with the Zn^{2+}-sensitive fluorophore of FluoZin-3 upon stimulation with AMPA [177]. It was proved that NW FETs modified with Aβ could interact with Zn^{2+} and show response to the extracellular Zn^{2+} released from stimulated neurons, which confirmed that Aβ and the Zn^{2+} homeostasis can be one of the diagnostic strategies for early detection of neurodegeneration.

An important indicator for cell viability is the extracellular and intracellular pH. To monitor cellular pH, SiNWs FETs were modified with a photoactive switchable molecular recognition layer, 8-hydroxypyrene-1,3,6-trisulfonyl chloride (HPTS), that can be optically switched between two chemically different states [176]. These two states have different acid dissociation constants and as a consequence affect the device surface potential to different extents. During sensing measurement, the ratio of the electrical signals measured in the two states were used for ratiometric internal calibration, thus eliminated the need for electrical calibration of individual devices. These NW FET devices were used for the monitoring cellular metabolic activity of Jurkat cells through the measurement of extracellular pH, which is determined by the excretion of acidic metabolites, such as CO_2, lactate and pyruvate. In addition, the growth kinetics and metabolic state of *Escherichia coli* (*E. coli*) cells in undiluted media was monitored by pH measurement using honeycomb-patterned SiNW FETs [178]. The time dependent profile of pH change for bacterial cultures were also used distinguish the effects of different types of antibiotics, which would allow assessment of antibiotic treatment durations by determining the needed time for a complete termination of the metabolic activity.

Nanowire arrays for in-vitro and in-vivo tissue electrophysiology

In-vitro tissue electrophysiology

The NW bioelectronics tools described above have demonstrated robust biochemical sensing as well as electrical recording from cultured cells. Yet the ultimate goal of understanding 3D cellular networks comprising tissues of, for example, the brain and heart, requires other considerations in the design of 'tissue-like' electronics. First, the fabrication approach of the NW devices based on one-on-one fabrication must be significantly scaled up to interrogate the highly innervated cellular networks [179]. Second, the substantially higher stiffness of conventional implantable electronics compared with soft tissues leads to chronic tissue damage and immune response [180] that has limited stable integration of bioelectronics with tissues. Third, the inherently 3D cellular networks of tissues defines the topology of electronics – 3D and macroporous – important for allowing interpenetration of cells and diffusion of biochemical species critical to tissue function [6]. The implementation of this paradigm has been achieved via seamless 3D integration of NW bioelectronics with synthetic tissues in vitro and live animals in vivo.

To push the limit of scalability of the NW arrays while maintaining their capability of probing 3D tissue networks, a recent study has developed a scalable approach to U-shaped SiNW arrays that combined deterministic shape-controlled NW assembly [181] and spatially defined semiconductor-to-metal transformation [182] to realize scalable NWFET probe arrays with controllable tip geometry and sensor size [179]. Specifically, the flexible NWs, with length-to-width ratio of more than 3000, were bent and aligned into thousands of 'U' shapes by 'combing' over thousands of U-shaped polymer trenches [181]. The center of each U-shaped NW, which eventually points upward from the wafer surface to interface the cells, is defined as a small FET recorder by controlled semiconductor-to-metal transformation [182] of the NW arms. After coating the NW surface with biomimetic phospholipid bilayer, the tips of the U-shaped devices can be inserted into the networks of targeted neurons and cardiomyocytes for parallel intracellular recording of signals up to or exceeding 100 mV which is comparable to the quality of those obtained by patch-clamp (Fig. 4a).

Along with the advancement of scalable NW device fabrication, studies have addressed all the key points of tissue interfacing and demonstrated organizing NW FETs within a 3D macroporous mesh structure similar to a tissue scaffold but with addressable active nanoelectronic devices [21]. The mesh structures were fabricated on a 2D substrate using a biocompatible polymer as the mesh ribbons, leaving the active NW devices exposed. After releasing from the substrate, the free-standing mesh structures were self-organized (with built strain) or mechanically deformed into 3D macroporous structures. The number and locations of the active devices were precisely defined during fabrication and assembly steps, and the mechanical properties of the mesh nanoelectronics were controlled by the structures of the polymer ribbons. The meshes were seeded with cardiac, neuron or human smooth muscle cells and co-cultured to produce synthetic tissues innervated in 3D with the NW FETs. Electrical recording data from the NWs showed the capability to record 3D action potential propagation in cardiac and neuronal hybrid tissues, as well as monitor pH changes in a vascular construct. More recently, a highly flexible and biocompatible macroporous mesh electronics have been designed for 3D cardiac cell culture [23].

The cardiac cells were seeded on 3D innervated structures formed by folding mesh electronic scaffolds with recording and stimulating nanodevices. Real-time quantitative mapping of action potential propagation in these macroporous engineered cardiac tissues with 64 channel NW FET recordings has been used to explore new directions, in situ tracing of 3D conducting pathways in developing cardiac tissues and probing the dynamics of action potential conduction in a transient arrhythmia disease model [23]. In addition, the incorporation of both FET sensors and stimulator devices has enabled precise control and rerouting of the action potential propagation directions. These results of high-temporal-resolution 3D electrophysiology mapping and manipulation in engineered cardiac tissues have the potential to impact cardiac research focused on drug-screening and the development of powerful cardiac 'patches' that can monitor and modulate the heart post-implantation [23].

In-vitro tissue electrophysiology

Introducing electronic probes into live animal tissue has been well-studied but also faced long-standing limitations as introduced above and recently the focus of much work [6,180,183,184]. To overcome these long-standing limitations of implantable electrode probes, a new paradigm has been introduced that uses syringe injection to deliver 3D macroporous mesh nanoelectronic networks into biological tissues (Fig. 4b) [6,22,185–187]. The ultra-flexible mesh electronics, which has mechanical modulus comparable to neural tissue, are first loaded into a glass needle and then partially injected into specific brain regions, the input/output interface left outside of the brain is then connected to standard measurement electronics [185,188]. Alternatively, the ultra-flexible 3D macroporous NW mesh probe can be frozen to temporarily enhance rigidity and rapidly inserted into the brain tissue [189]. In both cases, histology studies have shown that the brain implanted tissue-like mesh electronics probes do not elicit inflammatory immune response and show full tissue healing [6,185,186,189–191], in stark contrast to conventional probes. Consistent with the seamless immune-response-free tissue integration, implanted mesh electronics have demonstrated stable parallel tracking of single neuron and neural circuit activity for at least 8 months with stable monitoring and stimulation of the same groups of neurons, thus opening up new opportunities for understanding circuit plasticity, aging and neurodegenerative diseases [186,191].

Long-term stability of nanowires

Long-term applications in tissue electrophysiology, especially in vivo implants, require long-term stability of NW devices in physiological environments. For example, SiNWs have a native SiO_2 layer due to oxidation in air [192], and this oxide layer can be dissolved by hydrolysis. Cycles of re-oxidation and hydrolysis in aqueous solutions, where the hydrolysis rate is proportional to ionic strength, can lead to SiNW dissolution especially in high ionic strength physiological solutions [193,194]. As a result, the dissolution of nanoscale Si materials under physiological conditions has been observed between 1 and 3 weeks [21,129,195]. In addition, corrosion and degradation have also been reported for GaP NWs, which can not only cause failure of NW devices, but also leads to release of toxic Ga ions [196,197]. One commonly used method for enhancing NW stability involves introducing a stable conformal shell material [196,198–200]. For example, the long-term stability of 30 nm Si, Ge/Si and InAs NW devices in physiological environments can be improved from less than 10 days to over 100 days with a 10 nm thick conformal Al_2O_3 shell coating, without adversely affect the performance of NW FETs [198].

Another important consideration for chronic in vitro and in vivo interfaces is the biocompatibility of NWs incorporated onto substrates and free-standing NWs. For brain implants, the biggest challenge to be addressed is the chronic tissue damage and immune response [180]. Over time this damage and response can lead to reduced neuronal density and accumulation of glial cells near implants, thereby forming an insulating barrier at the electrode/neuron interface and causing unstable recording [180]. For vertical NW arrays on substrates, it was observed that they could promote neuronal growth and limit glial cell spreading [201]. Specifically, neurons cultured on NW arrays showed improved neurite outgrowth and long-term survival compared to neurons on standard culture substrates, presumably due to the improved adhesion of neurotrophic biomolecules on the NWs. The growth of glial cells, however, was suppressed by the presence of the NW arrays. Similarly, neurons cultured on carbon nanotubes on substrates also showed increased neurite growth [202,203]. In the case of free-standing NWs, only a few reports have addressed short-term inflammation [199,204]. Specifically, SiO_x-coated GaP NWs injected into rat striatum at a dose of 2.8×10^5 NWs/rat elicited astrocyte and microglia activation during the first week, which then declined over time. The SiO_x-coated NWs underwent partial degradation after 6 weeks and were engulfed by microglial cells by 12 weeks [199]. Another report compared the long-term brain tissue response to the degradable SiO_x-coated GaP NWs and non-degradable HfO_x-coated GaP NWs, and found that both types of NWs were engulfed by microglial cells [204]. No subacute or chronic toxicity was detected in these studies [199,204]. A potential complicating issue with the interpretation of these response is the fact that the time course of glial activation and engulfment is similar to that observed generically following brain tissue insult, either as a result of injection or implantation [205]. Last, in studies that compared long-term in vivo tissue response of both NWs and carbon nanotubes [206], NWs showed faster clearance rate by immune cells, and thus a shorter duration of inflammation response than carbon nanotubes. Taken together, these results open up opportunities for in vivo implant applications, where substrate-bound NWs and carbon nanotubes could possibly promote neuronal adhesion, survival and growth, and reduce chronic immune response [207]. To realize such advantages of substrate-bound materials, however, will require supporting probe structures that do not dominate the immune response in the brain [190].

Future perspectives

NW-based bioelectronics represent a new paradigm for seamlessly interfacing electronics with biological systems. With regard to biosensors, future research efforts focused on analyses of clinically relevant samples such as blood directly or with minimal sample preparation could have widespread impact from point-of-care diagnostics, including low-cost applications in underdeveloped nations, to real-time monitoring of critical care within hospitals. Further development of the concept of parallel sensing with NW sensor arrays to enable parallel detection of broad spectrum targets, including disease marker proteins, viruses and pathogens as well as DNA sequence variations, could lead to rapid and high-fidelity diagnoses for personalized medicine. However, several advancements should be achieved for NW biosensors to be translated into clinically useful diagnostic devices. First, diagnostic devices require routine manufacture with very little variability, and current synthetic control and fabrication methods of NWs should be improved to achieve scalable wafer-scale manufacture of reliable and uniform sensors [85]. Second, parallel sensing studies to date have only demonstrated detection of up to three antigens, though clinical applications of cancer diagnosis would often require high-throughput detection of tens or hundreds of biomarkers. Highly scalable fabrication and functionalization methods are required to significantly enhance the parallel detection capabilities, at the same time maintain high specificity to the targeted antigens.

With regard to NW platforms for studies of electrogenic cells, there remain a number of key directions in NW-based bioelectronics

research that could lead to transformative research advances in the life sciences. First, precise control of novel design and fabrication of multifunctional NW devices could lead to new understanding and interrogation of biosystems at an unprecedented scale. Second, further development of NW devices embedded in 3D tissue scaffold could enable monitoring and modulation of tissue development and building the platform for pharmacological screening and pathology studies. Third, incorporating NW FETs into the platform of mesh electronics to form synapse-like junctions with neurites [129] could allow for in vivo local field potential recording [208] and modulation. Further functionalizing NW devices with biomimetic cell-penetrating peptides [209] or receptors [61] or lipid bilayers [179] could also open up in vivo intracellular recording and/or chemical and biological detection [6,210]. To this end, studies have demonstrated strategies for achieving long-term stability of NW devices in physiological environments [198] and addressing the long-term tissue response [196,199] in the presence of NWs. Overall, the unique advantages of semiconductor NWs arrays and circuits will lead to artificial electronic networks that truly resemble the biological tissues, and thereby provide major opportunities in understanding complex biological systems in the near future and possibly drive high-resolution brain-machine interfaces in the more distant future [211].

CRediT authorship contribution statement

Anqi Zhang: Writing-original draft preparation. **Jae-Hyun Lee:** Visualization, Writing-reviewing and editing. **Charles M. Lieber:** Supervision, Writing-reviewing and editing, Funding acquisition.

Declaration of Competing Interest

The authors declare that they have no known competing financial interests or personal relationships that could have appeared to influence the work reported in this paper.

Acknowledgments

We thank the members of the Lieber lab for helpful discussions. C.M.L. acknowledges support of this work by the Air Force Office of Scientific Research (FA9550-18-1-0469, FA9550-19-1-0246) and a National Institutes of Health Director's Pioneer Award (1DP1EB025835-01). J.H.L. acknowledges support from the Institute for Basic Science (IBS-R026-D1).

References

[1] M. Bresadola, Medicine and science in the life of Luigi Galvani (1737–1798), Brain Res. Bull. 46 (1998) 367–380.
[2] A. Offenhäusser, R. Rinaldi, Nanobioelectronics-For Electronics, Biology, and Medicine, Springer, New York, 2009.
[3] A. Zhang, C.M. Lieber, Nano-bioelectronics, Chem. Rev. 116 (2016) 215–257.
[4] J. Wang, Electrochemical glucose biosensors, Chem. Rev. 108 (2008) 814–825.
[5] S.K. Mulpuru, M. Madhavan, C.J. McLeod, Y.-M. Cha, P.A. Friedman, Cardiac pacemakers: function, troubleshooting, and management, J. Am. Coll. Cardiol. 69 (2017) 189–210.
[6] G. Hong, X. Yang, T. Zhou, C.M. Lieber, Mesh electronics: a new paradigm for tissue-like brain probes, Curr. Opin. Neurobiol. 50 (2018) 33–41.
[7] X. Dai, G. Hong, T. Gao, C.M. Lieber, Mesh nanoelectronics: seamless integration of electronics with tissues, Acc. Chem. Res. 51 (2018) 309–318.
[8] M.E. Spira, A. Hai, Multi-electrode array technologies for neuroscience and cardiology, Nat. Nanotechnol. 8 (2013) 83–94.
[9] S. Kumar, R. Rani, N. Dilbaghi, K. Tankeshwar, K.-H. Kim, Carbon nanotubes: a novel material for multifaceted applications in human healthcare, Chem. Soc. Rev. 46 (2017) 158–196.
[10] C. Cheng, S. Li, A. Thomas, N.A. Kotov, R. Haag, Functional graphene nanomaterials based architectures: biointeractions, fabrications, and emerging biological applications, Chem. Rev. 117 (2017) 1826–1914.
[11] Z. Tu, G. Guday, M. Adeli, R. Haag, Multivalent interactions between 2D nanomaterials and biointerfaces, Adv. Mater. 30 (2018) 1706709.
[12] E. Zeglio, A.L. Rutz, T.E. Winkler, G.G. Malliaras, A. Herland, Conjugated polymers for assessing and controlling biological functions, Adv. Mater. 31 (2019) 1806712.
[13] S. Zhou, L. Nyholm, M. Strømme, Z. Wang, CladophoraCellulose: unique biopolymer nanofibrils for emerging energy, environmental, and life science applications, Acc. Chem. Res. 52 (2019) 2232–2243.
[14] A. Zhang, G. Zheng, C.M. Lieber, Nanowires: Building Blocks for Nanoscience and Nanotechnology, Springer, Switzerland, 2016.
[15] V. Schmidt, J. Wittemann, U. Gosele, Growth, thermodynamics, and electrical properties of silicon nanowires, Chem. Rev. 110 (2010) 361–388.
[16] A. Fontcuberta i Morral, S.A. Dayeh, C. Jagadish, Semiconductor Nanowires I: Growth and Theory, Academic Press, Waltham, MA, 2015.
[17] B. Tian, T. Cohen-Karni, Q. Qing, X. Duan, P. Xie, C.M. Lieber, Three-dimensional, flexible nanoscale field-effect transistors as localized bioprobes, Science 329 (2010) 830–834.
[18] J. Abbott, T. Ye, D. Ham, H. Park, Optimizing nanoelectrode arrays for scalable intracellular electrophysiology, Acc. Chem. Res. 51 (2018) 600–608.
[19] A.F. McGuire, F. Santoro, B. Cui, Interfacing cells with vertical nanoscale devices: applications and characterization, Annu. Rev. Anal. Chem. 11 (2018) 101–126.
[20] M.R. Angle, B. Cui, N.A. Melosh, Nanotechnology and neurophysiology, Curr. Opin. Neurobiol. 32 (2015) 132–140.
[21] B. Tian, J. Liu, T. Dvir, L. Jin, J.H. Tsui, Q. Qing, Z. Suo, R. Langer, D.S. Kohane, C.M. Lieber, Macroporous nanowire nanoelectronic scaffolds for synthetic tissues, Nat. Mater. 11 (2012) 986–994.
[22] J. Liu, T.-M. Fu, Z. Cheng, G. Hong, T. Zhou, L. Jin, M. Duvvuri, Z. Jiang, P. Kruskal, C. Xie, Z. Suo, Y. Fang, C.M. Lieber, Syringe-injectable electronics, Nat. Nanotechnol. 10 (2015) 629–636.
[23] X. Dai, W. Zhou, T. Gao, J. Liu, C.M. Lieber, Three-dimensional mapping and regulation of action potential propagation in nanoelectronics-innervated tissues, Nat. Nanotechnol. 11 (2016) 776–782.
[24] Z. Cheng, J. Hou, Q. Zhou, T. Li, H. Li, L. Yang, K. Jiang, C. Wang, Y. Li, Y. Fang, Sensitivity limits and scaling of bioelectronic graphene transducers, Nano Lett. 13 (2013) 2902–2907.
[25] B.-C. Zhang, H. Wang, L. He, C.-J. Zheng, J.-S. Jie, Y. Lifshitz, S.T. Lee, X.H. Zhang, Centimeter-long single-crystalline Si nanowires, Nano Lett. 17 (2017) 7323–7329.
[26] A.M. Morales, C.M. Lieber, A laser ablation method for the synthesis of crystalline semiconductor nanowires, Science 279 (1998) 208–211.
[27] E. Barrigón, M. Heurlin, Z. Bi, B. Monemar, L. Samuelson, Synthesis and applications of III–V nanowires, Chem. Rev. 119 (2019) 9170–9220.
[28] S.A. Dayeh, R. Chen, Y.G. Ro, J. Sim, Progress in doping semiconductor nanowires during growth, Mater. Sci. Semicond. Process. 62 (2017) 135–155.
[29] J. Wallentin, M.T. Borgström, Doping of semiconductor nanowires, J. Mater. Res. 26 (2011) 2142–2156.
[30] E.C. Garnett, Y.-C. Tseng, D.R. Khanal, J. Wu, J. Bokor, P. Yang, Dopant profiling and surface analysis of silicon nanowires using capacitance–voltage measurements, Nat. Nanotechnol. 4 (2009) 311–314.
[31] D.E. Perea, E.R. Hemesath, E.J. Schwalbach, J.L. Lensch-Falk, P.W. Voorhees, L.J. Lauhon, Direct measurement of dopant distribution in an individual vapour–liquid–solid nanowire, Nat. Nanotechnol. 4 (2009) 315–319.
[32] P. Xie, Y. Hu, Y. Fang, J. Huang, C.M. Lieber, Diameter-dependent dopant location in silicon and germanium nanowires, Proc. Natl. Acad. Sci. 106 (2009) 15254–15258.
[33] E. Koren, J. Hyun, U. Givan, E. Hemesath, L. Lauhon, Y. Rosenwaks, Obtaining uniform dopant distributions in VLS-grown Si nanowires, Nano Lett. 11 (2011) 183–187.
[34] C. Kendrick, M.-W. Kuo, J. Li, H. Shen, T.S. Mayer, J.M. Redwing, Uniform p-type doping of silicon nanowires synthesized via vapor-liquid-solid growth with silicon tetrachloride, J. Appl. Phys. 122 (2017) 235101.
[35] R. Agarwal, Heterointerfaces in semiconductor nanowires, Small 4 (2008) 1872–1893.
[36] J. Johansson, K.A. Dick, Recent advances in semiconductor nanowire heterostructures, CrystEngComm 13 (2011) 7175.
[37] C. Yang, Z. Zhong, C.M. Lieber, Encoding electronic properties by synthesis of axial modulation-doped silicon nanowires, Science 310 (2005) 1304–1307.
[38] A. Cavalli, J. Wang, I. Esmaeil Zadeh, M.E. Reimer, M.A. Verheijen, M. Soini, S.R. Plissard, V. Zwiller, J. Haverkort, E. Bakkers, High-yield growth and characterization of ⟨100⟩ InP p–n diode nanowires, Nano Lett. 16 (2016) 3071–3077.
[39] D.J. Hill, T.S. Teitsworth, S. Kim, J.D. Christesen, J.F. Cahoon, Encoding highly nonequilibrium boron concentrations and abrupt morphology in p-type/n-type silicon nanowire superlattices, ACS Appl. Mater. Interfaces 9 (2017) 37105–37111.
[40] Z. Luo, Y. Jiang, B.D. Myers, D. Isheim, J. Wu, J.F. Zimmerman, Z. Wang, Q. Li, Y. Wang, X. Chen, V.P. Dravid, D.N. Seidman, B. Tian, Atomic gold-enabled three-dimensional lithography for silicon mesostructures, Science 348 (2015) 1451–1455.
[41] S. Kim, D.J. Hill, C.W. Pinion, J.D. Christesen, J.R. McBride, J.F. Cahoon, Designing morphology in epitaxial silicon nanowires: the role of gold, surface chemistry, and phosphorus doping, ACS Nano 11 (2017) 4453–4462.
[42] R.W. Day, M.N. Mankin, R. Gao, Y.-S. No, S.-K. Kim, D.C. Bell, H.G. Park, C.M. Lieber, Plateau–Rayleigh crystal growth of periodic shells on one-dimensional substrates, Nat. Nanotechnol. 10 (2015) 345–352.
[43] B. Tian, P. Xie, T.J. Kempa, D.C. Bell, C.M. Lieber, Single-crystalline kinked semiconductor nanowire superstructures, Nat. Nanotechnol. 4 (2009) 824–829.
[44] Y. Shen, O.I. Lebedev, S. Turner, G. Van Tendeloo, X. Song, X. Yu, Q. Wang, H. Chen, S.A. Dayeh, T. Wu, Size-induced switching of nanowire growth direction: a new approach toward kinked nanostructures, Adv. Funct. Mater. 26 (2016) 3687–3695.
[45] F. Panciera, M.M. Norton, S.B. Alam, S. Hofmann, K. Mølhave, F.M. Ross, Controlling nanowire growth through electric field-induced deformation of the catalyst droplet, Nat. Commun. 7 (2016) 12271.

[46] Z. Sun, D.N. Seidman, L. Lauhon, Nanowire kinking modulates doping profiles by reshaping the liquid–solid growth interface, Nano Lett. 17 (2017) 4518–4525.
[47] T.A. Celano, D.J. Hill, X. Zhang, C.W. Pinion, J.D. Christesen, C.J. Flynn, J.R. McBride, J.F. Cahoon, Capillarity-driven welding of semiconductor nanowires for crystalline and electrically ohmic junctions, Nano Lett. 16 (2016) 5241–5246.
[48] A. Darbandi, J.C. McNeil, A. Akhtari-Zavareh, S.P. Watkins, K.L. Kavanagh, Direct measurement of the electrical abruptness of a nanowire p–n junction, Nano Lett. 16 (2016) 3982–3988.
[49] D.E. Perea, N. Li, R.M. Dickerson, A. Misra, S. Picraux, Controlling heterojunction abruptness in VLS-grown semiconductor nanowires via in situ catalyst alloying, Nano Lett. 11 (2011) 3117–3122.
[50] T. Cohen-Karni, D. Casanova, J.F. Cahoon, Q. Qing, D.C. Bell, C.M. Lieber, Synthetically encoded ultrashort-channel nanowire transistors for fast, point-like cellular signal detection, Nano Lett. 12 (2012) 2639–2644.
[51] K.A. Dick, J. Bolinsson, B.M. Borg, J. Johansson, Controlling the abruptness of axial heterojunctions in III–V nanowires: beyond the reservoir effect, Nano Lett. 12 (2012) 3200–3206.
[52] V. Zannier, F. Rossi, V.G. Dubrovskii, D. Ercolani, S. Battiato, L. Sorba, Nanoparticle stability in axial InAs–InP nanowire heterostructures with atomically sharp interfaces, Nano Lett. 18 (2018) 167–174.
[53] K.A. Dick, K. Deppert, L.S. Karlsson, M.W. Larsson, W. Seifert, L.R. Wallenberg, L. Samuelson, Directed growth of branched nanowire structures, MRS. Bull. 32 (2007) 127–133.
[54] D. Wang, F. Qian, C. Yang, Z. Zhong, C.M. Lieber, Rational growth of branched and hyperbranched nanowire structures, Nano Lett. 4 (2004) 871–874.
[55] K.A. Dick, K. Deppert, M.W. Larsson, T. Mårtensson, W. Seifert, L.R. Wallenberg, L. Samuelson, Synthesis of branched 'nanotrees' by controlled seeding of multiple branching events, Nat. Mater. 3 (2004) 380–384.
[56] X. Jiang, B. Tian, J. Xiang, F. Qian, G. Zheng, H. Wang, L. Mai, C.M. Lieber, Rational growth of branched nanowire heterostructures with synthetically encoded properties and function, Proc. Natl. Acad. Sci. 108 (2011) 12212–12216.
[57] X. Duan, R. Gao, P. Xie, T. Cohen-Karni, Q. Qing, H.S. Choe, B. Tian, X. Jiang, C.M. Lieber, Intracellular recordings of action potentials by an extracellular nanoscale field-effect transistor, Nat. Nanotechnol. 7 (2012) 174–179.
[58] L.J. Lauhon, M.S. Gudiksen, D. Wang, C.M. Lieber, Epitaxial core–shell and core–multishell nanowire heterostructures, Nature 420 (2002) 57–61.
[59] R.R. Zamani, F.S. Hage, S. Lehmann, Q.M. Ramasse, K.A. Dick, Atomic-resolution spectrum imaging of semiconductor nanowires, Nano Lett. 18 (2018) 1557–1563.
[60] R. Parameswaran, J.L. Carvalho-de-Souza, Y. Jiang, M.J. Burke, J.F. Zimmerman, K. Koehler, A.W. Phillips, J. Yi, E.J. Adams, F. Bezanilla, B. Tian, Photoelectrochemical modulation of neuronal activity with free-standing coaxial silicon nanowires, Nat. Nanotechnol. 13 (2018) 260–266.
[61] G. Zheng, F. Patolsky, Y. Cui, W.U. Wang, C.M. Lieber, Multiplexed electrical detection of cancer markers with nanowire sensor arrays, Nat. Biotechnol. 23 (2005) 1294–1301.
[62] L. Mu, I.A. Droujinine, J. Lee, M. Wipf, P. Davis, C. Adams, J. Hannant, M.A. Reed, Nanoelectronic platform for ultrasensitive detection of protein biomarkers in serum using DNA amplification, Anal. Chem. 89 (2017) 11325–11331.
[63] N. Gao, W. Zhou, X. Jiang, G. Hong, T.-M. Fu, C.M. Lieber, General strategy for biodetection in high ionic strength solutions using transistor-based nanoelectronic sensors, Nano Lett. 15 (2015) 2143–2148.
[64] Y. Cui, Q. Wei, H. Park, C.M. Lieber, Nanowire nanosensors for highly sensitive and selective detection of biological and chemical species, Science 293 (2001) 1289–1292.
[65] N. Misra, J.A. Martinez, S.-C.J. Huang, Y. Wang, P. Stroeve, C.P. Grigoropoulos, A. Noy, Bioelectronic silicon nanowire devices using functional membrane proteins, Proc. Natl. Acad. Sci. 106 (2009) 13780–13784.
[66] X. Chen, H. Zhang, R.H. Tunuguntla, A. Noy, Silicon nanoribbon pH sensors protected by a barrier membrane with carbon nanotube porins, Nano Lett. 19 (2019) 629–634.
[67] T.-W. Lin, P.-J. Hsieh, C.-L. Lin, Y.-Y. Fang, J.-X. Yang, C.-C. Tsai, P.L. Chiang, C.Y. Pan, Y.T. Chen, Label-free detection of protein-protein interactions using a calmodulin-modified nanowire transistor, Proc. Natl. Acad. Sci. 107 (2010) 1047–1052.
[68] E. Stern, J.F. Klemic, D.A. Routenberg, P.N. Wyrembak, D.B. Turner-Evans, A.D. Hamilton, D.A. LaVan, T.M. Fahmy, M.A. Reed, Label-free immunodetection with CMOS-compatible semiconducting nanowires, Nature 445 (2007) 519–522.
[69] J. Li, S. Pud, M. Petrychuk, A. Offenhausser, S. Vitusevich, Sensitivity enhancement of Si nanowire field effect transistor biosensors using single trap phenomena, Nano Lett. 14 (2014) 3504–3509.
[70] J.-i Hahm, C.M. Lieber, Direct ultrasensitive electrical detection of DNA and DNA sequence variations using nanowire nanosensors, Nano Lett. 4 (2004) 51.
[71] Z. Li, Y. Chen, X. Li, T. Kamins, K. Nauka, R.S. Williams, Sequence-specific label-free DNA sensors based on silicon nanowires, Nano Lett. 4 (2004) 245–247.
[72] Y.L. Bunimovich, Y.S. Shin, W.-S. Yeo, M. Amori, G. Kwong, J.R. Heath, Quantitative real-time measurements of DNA hybridization with alkylated nonoxidized silicon nanowires in electrolyte solution, J. Am. Chem. Soc. 128 (2006) 16323–16331.
[73] X. Wang, C.S. Ozkan, Multisegment nanowire sensors for the detection of DNA molecules, Nano Lett. 8 (2008) 398–404.
[74] A. Gao, N. Lu, P. Dai, T. Li, H. Pei, X. Gao, Y. Gong, Y. Wang, C. Fan, Silicon-nanowire-based CMOS-compatible field-effect transistor nanosensors for ultrasensitive electrical detection of nucleic acids, Nano Lett. 11 (2011) 3974–3978.
[75] F. Patolsky, G. Zheng, O. Hayden, M. Lakadamyali, X. Zhuang, C.M. Lieber, Electrical detection of single viruses, Proc. Natl. Acad. Sci. 101 (2004) 14017–14022.
[76] F. Shen, J. Wang, Z. Xu, Y. Wu, Q. Chen, X. Li, X. Jie, L. Li, M. Yao, X. Guo, T. Zhu, Rapid flu diagnosis using silicon nanowire sensor, Nano Lett. 12 (2012) 3722–3730.
[77] J. Li, G. He, H. Ueno, C. Jia, H. Noji, C. Qi, X. Guo, Direct real-time detection of single proteins using silicon nanowire-based electrical circuits, Nanoscale 8 (2016) 16172–16176.
[78] X. Duan, Y. Li, N.K. Rajan, D.A. Routenberg, Y. Modis, M.A. Reed, Quantification of the affinities and kinetics of protein interactions using silicon nanowire biosensors, Nat. Nanotechnol. 7 (2012) 401–407.
[79] C. Maedler, D. Kim, R.A. Spanjaard, M. Hong, S. Erramilli, P. Mohanty, Sensing of the melanoma biomarker TROY using silicon nanowire field-effect transistors, ACS Sens. 1 (2016) 696–701.
[80] J. Li, Y. Kutovyi, I. Zadorozhnyi, N. Boichuk, S. Vitusevich, Monitoring of dynamic processes during detection of cardiac biomarkers using silicon nanowire field-effect transistors, Adv. Mater. Interfaces 7 (2020) 2000508.
[81] M.-A. Doucey, S. Carrara, Nanowire sensors in cancer, Trends Biotechnol. 37 (2019) 86–99.
[82] G.-J. Zhang, K.T.C. Chai, H.Z.H. Luo, J.M. Huang, I.G.K. Tay, A.E.-J. Lim, M. Je, Multiplexed detection of cardiac biomarkers in serum with nanowire arrays using readout ASIC, Biosens. Bioelectron. 35 (2012) 218–223.
[83] N. Lu, A. Gao, P. Dai, H. Mao, X. Zuo, C. Fan, Y. Wang, T. Li, Ultrasensitive detection of dual cancer biomarkers with integrated CMOS-compatible nanowire arrays, Anal. Chem. 87 (2015) 11203–11208.
[84] A. Gao, X. Yang, J. Tong, L. Zhou, Y. Wang, J. Zhao, H. Mao, T. Li, Multiplexed detection of lung cancer biomarkers in patients serum with CMOS-compatible silicon nanowire arrays, Biosens. Bioelectron. 91 (2017) 482–488.
[85] S. Zafar, C. D'Emic, A. Jagtiani, E. Kratschmer, X. Miao, Y. Zhu, R. Mo, N. Sosa, H. Hamann, G. Shahidi, H. Riel, Silicon nanowire field effect transistor sensors with minimal sensor-to-sensor variations and enhanced sensing characteristics, ACS Nano 12 (2018) 6577–6587.
[86] S.P. Leong, W.W. Tseng, Micrometastatic cancer cells in lymph nodes, bone marrow, and blood: clinical significance and biologic implications: micrometastatic cancer cells, CA Cancer J. Clin. 64 (2014) 195–206.
[87] D.P. Tran, M.A. Winter, B. Wolfrum, R. Stockmann, C.-T. Yang, M. Pourhassan-Moghaddam, A. Offenhäusser, B. Thierry, Toward intraoperative detection of disseminated tumor cells in lymph nodes with silicon nanowire field effect transistors, ACS Nano 10 (2016) 2357–2364.
[88] H. Haick, Y.Y. Broza, P. Mochalski, V. Ruzsanyi, A. Amann, Assessment, origin, and implementation of breath volatile cancer markers, Chem. Soc. Rev. 43 (2014) 1423–1449.
[89] N. Shehada, G. Brönstrup, K. Funka, S. Christiansen, M. Leja, H. Haick, Ultrasensitive silicon nanowire for real-world gas sensing: noninvasive diagnosis of cancer from breath volatolome, Nano Lett. 15 (2015) 1288–1295.
[90] N. Shehada, J.C. Cancilla, J.S. Torrecilla, E.S. Pariente, G. Brönstrup, S. Christiansen, D.W. Johnson, M. Leja, M. Davies, O. Liran, N. Peled, H. Haick, Silicon nanowire sensors enable diagnosis of patients via exhaled breath, ACS Nano 10 (2016) 7047–7057.
[91] J. Becker, Signal transduction inhibitors—a work in progress, Nat. Biotechnol. 22 (2004) 15–18.
[92] W.U. Wang, C. Chen, K.-h Lin, Y. Fang, C.M. Lieber, Label-free detection of small-molecule-protein interactions by using nanowire nanosensors, Proc. Natl. Acad. Sci. 102 (2005) 3208–3212.
[93] N. Elfström, R. Juhasz, I. Sychugov, T. Engfeldt, A.E. Karlström, J. Linnros, Surface charge sensitivity of silicon nanowires: size dependence, Nano Lett. 7 (2007) 2608–2612.
[94] K. Kim, C. Park, D. Kwon, D. Kim, M. Meyyappan, S. Jeon, J.S. Lee, Silicon nanowire biosensors for detection of cardiac troponin I (cTnI) with high sensitivity, Biosens. Bioelectron. 77 (2016) 695–701.
[95] M.-L. Seol, J.-H. Ahn, J.-M. Choi, S.-J. Choi, Y.-K. Choi, Self-aligned nanoforest in silicon nanowire for sensitive conductance modulation, Nano Lett. 12 (2012) 5603–5608.
[96] P.R. Nair, M.A. Alam, Design considerations of silicon nanowire biosensors, IEEE Trans. Electron Devices 54 (2007) 3400–3408.
[97] B. Dorvel, B. Reddy Jr., R. Bashir, Effect of biointerfacing linker chemistries on the sensitivity of silicon nanowires for protein detection, Anal. Chem. 85 (2013) 9493–9500.
[98] J. Li, Y. Zhang, S. To, L. You, Y. Sun, Effect of nanowire number, diameter, and doping density on nano-FET biosensor sensitivity, ACS Nano 5 (2011) 6661–6668.
[99] E. Stern, R. Wagner, F.J. Sigworth, R. Breaker, T.M. Fahmy, M.A. Reed, Importance of the Debye screening length on nanowire field effect transistor sensors, Nano Lett. 7 (2007) 3405–3409.
[100] I. Park, Z. Li, A.P. Pisano, R.S. Williams, Selective surface functionalization of silicon nanowires via nanoscale joule heating, Nano Lett. 7 (2007) 3106–3111.
[101] M. Masood, S. Chen, E. Carlen, A.v.d Berg, All-(111) surface silicon nanowires: selective functionalization for biosensing applications, ACS Appl. Mater. Interfaces 2 (2010) 3422–3428.
[102] B.-R. Li, C.-W. Chen, W.-L. Yang, T.-Y. Lin, C.-Y. Pan, Y.-T. Chen, Biomolecular recognition with a sensitivity-enhanced nanowire transistor biosensor, Biosens. Bioelectron. 45 (2013) 252–259.
[103] H.H. Liu, T.H. Lin, J.-T. Sheu, Self-assembled monolayer-based selective modification on polysilicon nanobelt devices, ACS Appl. Mater. Interfaces 5 (2013) 10048–10053.
[104] J. Veerbeek, R. Steen, W. Vijselaar, W.F. Rurup, S. Korom, A. Rozzi, R. Corradini, L. Segerink, J. Huskens, Selective functionalization with PNA of silicon nanowires on silicon oxide substrates, Langmuir 34 (2018) 11395–11404.

[105] C.-J. Chu, C.-S. Yeh, C.-K. Liao, L.-C. Tsai, C.-M. Huang, H.-Y. Lin, J.J. Shyue, Y.T. Chen, C.D. Chen, Improving nanowire sensing capability by electrical field alignment of surface probing molecules, Nano Lett. 13 (2013) 2564–2569.
[106] T. Shimada, T. Yasui, A. Yokoyama, T. Goda, M. Hara, T. Yanagida, N. Kaji, M. Kanai, K. Nagashima, Y. Miyahara, T. Kawai, Y. Baba, Biomolecular recognition on nanowire surfaces modified by the self-assembled monolayer, Lab Chip 18 (2018) 3225–3229.
[107] D.-S. Su, P.-Y. Chen, H.-C. Chiu, C.-C. Han, T.-J. Yen, H.-M. Chen, Photoelectrochemical biosensor for 5hmC detection based on the photocurrent inhibition effect of ZnO on MoS2/C3N4 heterojunction, Biosens. Bioelectron. 142 (2019) 111516–111544.
[108] A. Gao, N. Zou, P. Dai, N. Lu, T. Li, Y. Wang, J. Zhao, H. Mao, Signal-to-noise ratio enhancement of silicon nanowires biosensor with rolling circle amplification, Nano Lett. 13 (2013) 4123–4130.
[109] S.M. Sze, K.K. Ng, Physics of Semiconductor Devices, John Wiley & Sons, New Jersey, 2006.
[110] X.P. Gao, G. Zheng, C.M. Lieber, Subthreshold regime has the optimal sensitivity for nanowire FET biosensors, Nano Lett. 10 (2010) 547–552.
[111] M. Majumder, M. Alvi, M. Islam, M. Najmussadat, R. Islam, Sensitivity analysis of nanowire biosensor in the partially depleted and fully depleted mode of subthreshold region, Sens. Bio-Sens. Res. 7 (2016) 55–61.
[112] J.N. Israelachvili, Intermolecular and Surface Forces: With Applications to Colloidal and Biological Systems, Academic Press, London, 1985.
[113] E. Stern, A. Vacic, N.K. Rajan, J.M. Criscione, J. Park, B.R. Ilic, D.J. Mooney, M.A. Reed, T.M. Fahmy, Label-free biomarker detection from whole blood, Nat. Nanotechnol. 5 (2010) 138–142.
[114] H. Chen, X. Zhao, Z. Xi, Y. Zhang, H. Li, Z. Li, H. Shi, L. Huang, R. Shen, J. Tao, T. Wang, A new biosensor detection system to overcome the Debye screening effect: dialysis-silicon nanowire field effect transistor, IJN 14 (2019) 2985–2993.
[115] B.-R. Li, Y.-J. Hsieh, Y.-X. Chen, Y.-T. Chung, C.-Y. Pan, Y.-T. Chen, An ultrasensitive nanowire-transistor biosensor for detecting dopamine release from living PC12 cells under hypoxic stimulation, J. Am. Chem. Soc. 135 (2013) 16034–16037.
[116] A. Anand, C.-R. Liu, A.-C. Chou, W.-H. Hsu, R.K. Ulaganathan, Y.-C. Lin, C.A. Dai, F.G. Tseng, C.Y. Pan, Y.T. Chen, Detection of K+ efflux from stimulated cortical neurons by an aptamer-modified silicon nanowire field-effect transistor, ACS Sens. 2 (2017) 69–79.
[117] C.-A. Vu, W.-P. Hu, Y.-S. Yang, H.W.-H. Chan, W.-Y. Chen, Signal enhancement of silicon nanowire field-effect transistor immunosensors by RNA aptamer, ACS Omega 4 (2019) 14765–14771.
[118] R. Elnathan, M. Kwiat, A. Pevzner, Y. Engel, L. Burstein, A. Khatchtourints, A. Lichtenstein, R. Kantaev, F. Patolsky, Biorecognition layer engineering: overcoming screening limitations of nanowire-based FET devices, Nano Lett. 12 (2012) 5245–5254.
[119] N. Nakatsuka, K.-A. Yang, J.M. Abendroth, K.M. Cheung, X. Xu, H. Yang, C. Zhao, B. Zhu, Y.S. Rim, Y. Yang, P.S. Weiss, M.N. Stojanović, A.M. Andrews, Aptamer–field-effect transistors overcome Debye length limitations for small-molecule sensing, Science 362 (2018) 319–324.
[120] C.-A. Vu, W.-Y. Chen, Y.-S. Yang, H.W.-H. Chan, Improved biomarker quantification of silicon nanowire field-effect transistor immunosensors with signal enhancement by RNA aptamer: amyloid beta as a case study, Sens. Actuators B Chem. 329 (2021) 129150, https://doi.org/10.1016/j.snb.2020.129150
[121] G.S. Kulkarni, Z. Zhong, Detection beyond the Debye screening length in a high-frequency nanoelectronic biosensor, Nano Lett. 12 (2012) 719–723.
[122] M. Crescentini, M. Rossi, P. Ashburn, M. Lombardini, E. Sangiorgi, H. Morgan, M. Tartagni, AC and phase sensing of nanowires for biosensing, Biosensors 6 (2016) 15.
[123] E. Piccinini, S. Alberti, G.S. Longo, T. Berninger, J. Breu, J. Dostalek, O. Azzaroni, W. Knoll, Pushing the boundaries of interfacial sensitivity in graphene FET sensors: polyelectrolyte multilayers strongly increase the debye screening length, J. Phys. Chem. C 122 (2018) 10181–10188.
[124] R. Janissen, P.K. Sahoo, C.A. Santos, A.M. da Silva, A.A.G. von Zuben, D.E.P. Souto, A. Costa, P. Celedon, N. Zanchin, D.B. Almeida, D.S. Oliveira, L.T. Kubota, C.L. Cesar, A. Souza, M.A. Cotta, InP nanowire biosensor with tailored biofunctionalization: ultrasensitive and highly selective disease biomarker detection, Nano Lett. 17 (2017) 5938–5949.
[125] V. Krivitsky, M. Zverzhinetsky, F. Patolsky, Antigen-dissociation from antibody-modified nanotransistor sensor arrays as a direct biomarker detection method in unprocessed biosamples, Nano Lett. 16 (2016) 6272–6281.
[126] A. Molleman, Patch Clamping: An Introductory Guide to Patch Clamp Electrophysiology, John Wiley & Sons, Chichester, England, 2003.
[127] P.B. Kruskal, Z. Jiang, T. Gao, C.M. Lieber, Beyond the patch clamp: nanotechnologies for intracellular recording, Neuron 86 (2015) 21–24.
[128] B. Tian, C.M. Lieber, Synthetic nanoelectronic probes for biological cells and tissues, Annu. Rev. Anal. Chem. 6 (2013) 31–51.
[129] F. Patolsky, Detection, stimulation, and inhibition of neuronal signals with high-density nanowire transistor arrays, Science 313 (2006) 1100–1104.
[130] F. Santoro, S. Dasgupta, J. Schnitker, T. Auth, E. Neumann, G. Panaitov, G. Gompper, A. Offenhäusser, Interfacing electrogenic cells with 3D nanoelectrodes: position, shape, and size matter, ACS Nano 8 (2014) 6713–6723.
[131] A. Hai, J. Shappir, M.E. Spira, Long-term, multisite, parallel, in-cell recording and stimulation by an array of extracellular microelectrodes, J. Neurophysiol. 104 (2010) 559–568.
[132] F. Santoro, W. Zhao, L.-M. Joubert, L. Duan, J. Schnitker, Y. van de Burgt, H.Y. Lou, B. Liu, A. Salleo, L. Cui, Y. Cui, B. Cui, Revealing the cell–material interface with nanometer resolution by focused ion beam/scanning electron microscopy, ACS Nano 11 (2017) 8320–8328.
[133] A. Cohen, J. Shappir, S. Yitzchaik, M.E. Spira, Reversible transition of extracellular field potential recordings to intracellular recordings of action potentials generated by neurons grown on transistors, Biosens. Bioelectron. 23 (2008) 811–819.
[134] T. Cohen-Karni, B.P. Timko, L.E. Weiss, C.M. Lieber, Flexible electrical recording from cells using nanowire transistor arrays, Proc. Natl. Acad. Sci. 106 (2009) 7309–7313.
[135] T.-S. Pui, A. Agarwal, F. Ye, N. Balasubramanian, P. Chen, CMOS-compatible nanowire sensor arrays for detection of cellular bioelectricity, Small 5 (2009) 208–212.
[136] J.F. Eschermann, R. Stockmann, M. Hueske, X.T. Vu, S. Ingebrandt, A. Offenhäusser, Action potentials of HL-1 cells recorded with silicon nanowire transistors, Appl. Phys. Lett. 95 (2009) 083703.
[137] I. Zadorozhnyi, H. Hlukhova, Y. Kutovyi, V. Handziuk, N. Naumova, A. Offenhaeusser, S. Vitusevich, Towards pharmacological treatment screening of cardiomyocyte cells using Si nanowire FETs, Biosens. Bioelectron. 137 (2019) 229–235.
[138] J.-H. Lee, E.-J. Chae, S.-j Park, J.-W. Choi, Label-free detection of γ-aminobutyric acid based on silicon nanowire biosensor, Nano Converg. 6 (2019) 13.
[139] L. Zhao, H. Li, J. Meng, A.C. Wang, P. Tan, Y. Zou, et al., Adv. Funct. Mater. (2019) 1907999.
[140] G.W. Arbuthnott, J. Wickens, Space, time and dopamine, Trends Neurosci. 30 (2007) 62–69.
[141] E. Saracino, L. Maiolo, D. Polese, M. Semprini, A.I. Borrachero-Conejo, J. Gasparetto, S. Murtagh, M. Sola, L. Tomasi, F. Valle, L. Pazzini, F. Formaggio, M. Chiappalone, S. Hussain, M. Caprini, M. Muccini, L. Ambrosio, G. Fortunato, R. Zamboni, A. Convertino, V. Benfenati, A glial-silicon nanowire electrode junction enabling differentiation and noninvasive recording of slow oscillations from primary astrocytes, Adv. Biosyst. 4 (2020) 1900264.
[142] Q. Qing, Z. Jiang, L. Xu, R. Gao, L. Mai, C.M. Lieber, Free-standing kinked nanowire transistor probes for targeted intracellular recording in three dimensions, Nat. Nanotechnol. 9 (2014) 142–147.
[143] Y. Zhang, J. Clausmeyer, B. Babakinejad, A. López Córdoba, T. Ali, A. Shevchuk, Y. Takahashi, P. Novak, C. Edwards, M. Lab, S. Gopal, C. Chiappini, U. Anand, L. Magnani, R.C. Coombes, J. Gorelik, T. Matsue, W. Schuhmann, D. Klenerman, E.V. Sviderskaya, Y. Korchev, Spearhead nanometric field-effect transistor sensors for single-cell analysis, ACS Nano 10 (2016) 3214–3221.
[144] T. Berthing, S. Bonde, K.R. Rostgaard, M.H. Madsen, C.B. Sørensen, J. Nygård, K.L. Martinez, Cell membrane conformation at vertical nanowire array interface revealed by fluorescence imaging, Nanotechnology 23 (2012) 415102.
[145] F. Santoro, W. Zhao, L.-M. Joubert, L. Duan, J. Schnitker, Y. van de Burgt, H.Y. Lou, B. Liu, A. Salleo, L. Cui, Y. Cui, B. Cui, Revealing the cell–material interface with nanometer resolution by focused ion beam/scanning electron microscopy, ACS Nano 11 (2017) 8320–8328.
[146] G. He, N. Hu, A.M. Xu, X. Li, Y. Zhao, X. Xie, Nanoneedle platforms: the many ways to pierce the cell membrane, Adv. Funct. Mater. 30 (2020) 1909890.
[147] R. Liu, R. Chen, A.T. Elthakeb, S.H. Lee, S. Hinckley, M.L. Khraiche, J. Scott, D. Pre, Y. Hwang, A. Tanaka, Y.G. Ro, A.K. Matsushita, X. Dai, C. Soci, S. Biesmans, A. James, J. Nogan, K.L. Jungjohann, D.V. Pete, D.B. Webb, Y. Zou, A.G. Bang, S.A. Dayeh, High density individually addressable nanowire arrays record intracellular activity from primary rodent and human stem cell derived neurons, Nano Lett. 17 (2017) 2757–2764.
[148] J. Yoo, H. Kwak, J. Kwon, G.E. Ha, E.H. Lee, S. Song, J. Na, H.J. Lee, J. Lee, A. Hwangbo, E. Cha, Y. Chae, E. Cheong, H.J. Choi, Long-term intracellular recording of optogenetically-induced electrical activities using vertical nanowire multi electrode array, Sci. Rep. 10 (2020) 4279.
[149] A.M. Xu, A. Aalipour, S. Leal-Ortiz, A.H. Mekhdjian, X. Xie, A.R. Dunn, C.C. Garner, N.A. Melosh, Quantification of nanowire penetration into living cells, Nat. Commun. 5 (2014) 3613.
[150] M. Dipalo, A.F. McGuire, H.-Y. Lou, V. Caprettini, G. Melle, G. Bruno, C. Lubrano, L. Matino, X. Li, F. De Angelis, B. Cui, F. Santoro, Cells adhering to 3D vertical nanostructures: cell membrane reshaping without stable internalization, Nano Lett. 18 (2018) 6100–6105.
[151] R. Capozza, V. Caprettini, C.A. Gonano, A. Bosca, F. Moia, F. Santoro, F. De Angelis, Cell membrane disruption by vertical micro-/nanopillars: role of membrane bending and traction forces, ACS Appl. Mater. Interfaces 10 (2018) 29107–29114.
[152] J.T. Robinson, M. Jorgolli, A.K. Shalek, M.-H. Yoon, R.S. Gertner, H. Park, Vertical nanowire electrode arrays as a scalable platform for intracellular interfacing to neuronal circuits, Nat. Nanotechnol. 7 (2012) 180–184.
[153] C. Xie, Z. Lin, L. Hanson, Y. Cui, B. Cui, Intracellular recording of action potentials by nanopillar electroporation, Nat. Nanotechnol. 7 (2012) 185–190.
[154] Z.C. Lin, C. Xie, Y. Osakada, Y. Cui, B. Cui, Iridium oxide nanotube electrodes for sensitive and prolonged intracellular measurement of action potentials, Nat. Commun. 5 (2014) 3206.
[155] Z.C. Lin, A.F. McGuire, P.W. Burridge, E. Matsa, H.-Y. Lou, J.C. Wu, B. Cui, Accurate nanoelectrode recording of human pluripotent stem cell-derived cardiomyocytes for assaying drugs and modeling disease, Microsyst. Nanoeng. 3 (2017) 16080.
[156] J. Abbott, T. Ye, L. Qin, M. Jorgolli, R.S. Gertner, D. Ham, H. Park, CMOS nanoelectrode array for all-electrical intracellular electrophysiological imaging, Nat. Nanotechnol. 12 (2017) 460–466.
[157] H. Liu, O.A. Bolonduro, N. Hu, J. Ju, A.A. Rao, B.M. Duffy, Z. Huang, L.D. Black, B.P. Timko, Heart-on-a-chip model with integrated extra- and intracellular bioelectronics for monitoring cardiac electrophysiology under acute hypoxia, Nano Lett. 20 (2020) 2585–2593.
[158] A.-R. Shokouhi, S. Aslanoglou, D. Nisbet, N.H. Voelcker, R. Elnathan, Vertically configured nanostructure-mediated electroporation: a promising route for intracellular regulations and interrogations, Mater. Horiz. 7 (2020) 2810–2831.

[159] H. Liu, O.A. Bolonduro, N. Hu, J. Ju, A.A. Rao, B.M. Duffy, Z. Huang, L.D. Black, B.P. Timko, Heart-on-a-chip model with integrated extra- and intracellular bioelectronics for monitoring cardiac electrophysiology under acute hypoxia, Nano Lett. 20 (2020) 2585–2593.
[160] M. Dipalo, H. Amin, L. Lovato, F. Moia, V. Caprettini, G.C. Messina, F. Tantussi, L. Berdondini, F. De Angelis, Intracellular and extracellular recording of spontaneous action potentials in mammalian neurons and cardiac cells with 3D plasmonic nanoelectrodes, Nano Lett. 17 (2017) 3932–3939.
[161] M. Dipalo, G. Melle, L. Lovato, A. Jacassi, F. Santoro, V. Caprettini, A. Schirato, A. Alabastri, D. Garoli, G. Bruno, F. Tantussi, F. De Angelis, Plasmonic meta-electrodes allow intracellular recordings at network level on high-density CMOS-multi-electrode arrays, Nat. Nanotechnol. 13 (2018) 965–971.
[162] M. Dipalo, V. Caprettini, G. Bruno, F. Caliendo, L.D. Garma, G. Melle, M. Dukhinova, V. Siciliano, F. Santoro, F. De Angelis, Membrane poration mechanisms at the cell–nanostructure interface, Adv. Biosyst. 3 (2019) 1900148.
[163] M. Dipalo, H. Amin, L. Lovato, F. Moia, V. Caprettini, G.C. Messina, F. Tantussi, L. Berdondini, F. De Angelis, Intracellular and extracellular recording of spontaneous action potentials in mammalian neurons and cardiac cells with 3D plasmonic nanoelectrodes, Nano Lett. 17 (2017) 3932–3939.
[164] B.D. Almquist, N.A. Melosh, Fusion of biomimetic stealth probes into lipid bilayer cores, Proc. Natl. Acad. Sci. 107 (2010) 5815–5820.
[165] B.X.E. Desbiolles, E. de Coulon, A. Bertsch, S. Rohr, P. Renaud, Intracellular recording of cardiomyocyte action potentials with nanopatterned volcano-shaped microelectrode arrays, Nano Lett. 19 (2019) 6173–6181.
[166] J. Abbott, T. Ye, K. Krenek, R.S. Gertner, S. Ban, Y. Kim, et al., Nat. Biomed. Eng. (2019) 1.
[167] L. Guo, On neural recording using nanoprotrusion electrodes, J. Neural Eng. 17 (2019) 016017.
[168] R. Parameswaran, K. Koehler, M.Y. Rotenberg, M.J. Burke, J. Kim, K.-Y. Jeong, B. Hissa, M.D. Paul, K. Moreno, N. Sarma, T. Hayes, E. Sudzilovsky, H.G. Park, B. Tian, Optical stimulation of cardiac cells with a polymer-supported silicon nanowire matrix, Proc. Natl. Acad. Sci. USA 116 (2019) 413–421.
[169] M.Y. Rotenberg, B. Elbaz, V. Nair, E.N. Schaumann, N. Yamamoto, N. Sarma, L. Matino, F. Santoro, B. Tian, Silicon nanowires for intracellular optical interrogation with subcellular resolution, Nano Lett. 20 (2020) 1226–1232.
[170] Y. Jiang, X. Li, B. Liu, J. Yi, Y. Fang, F. Shi, X. Gao, E. Sudzilovsky, R. Parameswaran, K. Koehler, V. Nair, J. Yue, K. Guo, Y. Fang, H.M. Tsai, G. Freyermuth, R. Wong, C.M. Kao, C.T. Chen, A.W. Nicholls, X. Wu, G. Shepherd, B. Tian, Rational design of silicon structures for optically controlled multiscale biointerfaces, Nat. Biomed. Eng. 2 (2018) 508–521.
[171] Y. Fang, Y. Jiang, H. Acaron Ledesma, J. Yi, X. Gao, D.E. Weiss, F. Shi, B. Tian, Texturing silicon nanowires for highly localized optical modulation of cellular dynamics, Nano Lett. 18 (2018) 4487–4492.
[172] E.S. Boyden, F. Zhang, E. Bamberg, G. Nagel, K. Deisseroth, Millisecond-timescale, genetically targeted optical control of neural activity, Nat. Neurosci. 8 (2005) 1263–1268.
[173] Y. Jiang, R. Parameswaran, X. Li, J.L. Carvalho-de-Souza, X. Gao, L. Meng, F. Bezanilla, G. Shepherd, B. Tian, Nongenetic optical neuromodulation with silicon-based materials, Nat. Protoc. 14 (2019) 1339–1376.
[174] J. Tang, N. Qin, Y. Chong, Y. Diao, Z. Yiliguma, Z. Wang, T. Xue, M. Jiang, J. Zhang, G. Zheng, Nanowire arrays restore vision in blind mice, Nat. Commun. 9 (2018) 786.
[175] K.-S. Chang, C.-J. Sun, P.-L. Chiang, A.-C. Chou, M.-C. Lin, C. Liang, H.H. Hung, Y.H. Yeh, C.D. Chen, C.Y. Pan, Y.T. Chen, Monitoring extracellular K+ flux with a valinomycin-coated silicon nanowire field-effect transistor, Biosens. Bioelectron. 31 (2012) 137–143.
[176] H. Peretz-Soroka, A. Pevzner, G. Davidi, V. Naddaka, R. Tirosh, E. Flaxer, F. Patolsky, Optically-gated self-calibrating nanosensors: monitoring pH and metabolic activity of living cells, Nano Lett. 13 (2013) 3157–3168.
[177] A. Anand, C.H. Chi, S. Banerjee, M.Y. Chou, F.G. Tseng, C.Y. Pan, Y.T. Chen, The extracellular Zn2+ concentration surrounding excited neurons is high enough to bind amyloid-β revealed by a nanowire transistor, Small 14 (2018) 1704439.
[178] B. Ibarlucea, T. Rim, C. Baek, J. De Visser, L. Baraban, G. Cuniberti, Nanowire sensors monitor bacterial growth kinetics and response to antibiotics, Lab Chip 17 (2017) 4283–4293.
[179] Y. Zhao, S.S. You, A. Zhang, J.-H. Lee, J. Huang, C.M. Lieber, Scalable ultrasmall three-dimensional nanowire transistor probes for intracellular recording, Nat. Nanotechnol. 14 (2019) 783–790.
[180] R. Chen, A. Canales, P. Anikeeva, Neural recording and modulation technologies, Nat. Rev. Mater. 2 (2017) 16093.
[181] Y. Zhao, J. Yao, L. Xu, M.N. Mankin, Y. Zhu, H. Wu, L. Mai, Q. Zhang, C.M. Lieber, Shape-controlled deterministic assembly of nanowires, Nano Lett. 16 (2016) 2644–2650.
[182] Y. Wu, J. Xiang, C. Yang, W. Lu, C.M. Lieber, Single-crystal metallic nanowires and metal/semiconductor nanowire heterostructures, Nature 430 (2004) 61–65.
[183] R. Feiner, T. Dvir, Tissue–electronics interfaces: from implantable devices to engineered tissues, Nat. Rev. Mater. 3 (2017) 17076.
[184] V.S. Polikov, P.A. Tresco, W.M. Reichert, Response of brain tissue to chronically implanted neural electrodes, J. Neurosci. Methods 148 (2005) 1–18.
[185] G. Hong, T.-M. Fu, T. Zhou, T.G. Schuhmann, J. Huang, C.M. Lieber, Syringe injectable electronics: precise targeted delivery with quantitative input/output connectivity, Nano Lett. 15 (2015) 6979–6984.
[186] T.-M. Fu, G. Hong, T. Zhou, T.G. Schuhmann, R.D. Viveros, C.M. Lieber, Stable long-term chronic brain mapping at the single-neuron level, Nat. Methods 13 (2016) 875–882.
[187] X. Yang, T. Zhou, T.J. Zwang, G. Hong, Y. Zhao, R.D. Viveros, T.M. Fu, T. Gao, C.M. Lieber, Bioinspired neuron-like electronics, Nat. Mater. 18 (2019) 510–517.
[188] T.G. Schuhmann, J. Yao, G. Hong, T.-M. Fu, C.M. Lieber, Syringe-injectable electronics with a plug-and-play input/output interface, Nano Lett. 17 (2017) 5836–5842.
[189] C. Xie, J. Liu, T.-M. Fu, X. Dai, W. Zhou, C.M. Lieber, Three-dimensional macroporous nanoelectronic networks as minimally invasive brain probes, Nat. Mater. 14 (2015) 1286–1292.
[190] T. Zhou, G. Hong, T.-M. Fu, X. Yang, T.G. Schuhmann, R.D. Viveros, C.M. Lieber, Syringe-injectable mesh electronics integrate seamlessly with minimal chronic immune response in the brain, Proc. Natl. Acad. Sci. USA 114 (2017) 5894–5899.
[191] T.-M. Fu, G. Hong, R.D. Viveros, T. Zhou, C.M. Lieber, Highly scalable multichannel mesh electronics for stable chronic brain electrophysiology, Proc. Natl. Acad. Sci. USA 114 (2017) E10046–E10055.
[192] Y. Cui, L.J. Lauhon, M.S. Gudiksen, J. Wang, C.M. Lieber, Diameter-controlled synthesis of single-crystal silicon nanowires, Appl. Phys. Lett. 78 (2001) 2214–2216.
[193] J.D. Rimstidt, H. Barnes, The kinetics of silica-water reactions, Geochim. Cosmochim. Acta 44 (1980) 1683–1699.
[194] P.V. Brady, J.V. Walther, Kinetics of quartz dissolution at low temperatures, Chem. Geol. 82 (1990) 253–264.
[195] S.-W. Hwang, H. Tao, D.-H. Kim, H. Cheng, J.-K. Song, E. Rill, M.A. Brenckle, B. Panilaitis, S.M. Won, Y.S. Kim, Y.M. Song, K.J. Yu, A. Ameen, R. Li, Y. Su, M. Yang, D.L. Kaplan, M.R. Zakin, M.J. Slepian, Y. Huang, F.G. Omenetto, J.A. Rogers, A physically transient form of silicon electronics, Science 337 (2012) 1640–1644.
[196] L. Gällentoft, L.M. Pettersson, N. Danielsen, J. Schouenborg, C.N. Prinz, C.E. Linsmeier, Impact of degradable nanowires on long-term brain tissue responses, J. Nanobiotechnol. 14 (2016) 64.
[197] D. Richards, D. Zemlyanov, A. Ivanisevic, Assessment of the passivation capabilities of two different covalent chemical modifications on GaP(100), Langmuir 26 (2010) 8141–8146.
[198] W. Zhou, X. Dai, T.-M. Fu, C. Xie, J. Liu, C.M. Lieber, Long term stability of nanowire nanoelectronics in physiological environments, Nano Lett. 14 (2014) 1614–1619.
[199] C. Eriksson Linsmeier, C.N. Prinz, L.M.E. Pettersson, P. Caroff, L. Samuelson, J. Schouenborg, L. Montelius, N. Danielsen, Nanowire biocompatibility in the brain – looking for a needle in a 3D stack, Nano Lett. 9 (2009) 4184–4190.
[200] L. Gällentoft, L.M. Pettersson, N. Danielsen, J. Schouenborg, C.N. Prinz, C.E. Linsmeier, Size-dependent long-term tissue response to biostable nanowires in the brain, Biomaterials 42 (2015) 172–183.
[201] G. Piret, M.-T. Perez, C.N. Prinz, Neurite outgrowth and synaptophysin expression of postnatal CNS neurons on GaP nanowire arrays in long-term retinal cell culture, Biomaterials 34 (2013) 875–887.
[202] M.P. Mattson, R.C. Haddon, A.M. Rao, Molecular functionalization of carbon nanotubes and use as substrates for neuronal growth, JMN 14 (2000) 175–182.
[203] E.B. Malarkey, K.A. Fisher, E. Bekyarova, W. Liu, R.C. Haddon, V. Parpura, Conductive single-walled carbon nanotube substrates modulate neuronal growth, Nano Lett. 9 (2009) 264–268.
[204] L. Gällentoft, L.M. Pettersson, N. Danielsen, J. Schouenborg, C.N. Prinz, C.E. Linsmeier, Impact of degradable nanowires on long-term brain tissue responses, J. Nanobiotechnol. 14 (2016) 64.
[205] G. Hong, C.M. Lieber, Novel electrode technologies for neural recordings, Nat. Rev. Neurosci. 20 (2019) 330–345.
[206] J.R. Roberts, R.R. Mercer, R.S. Chapman, G.M. Cohen, S. Bangsaruntip, D. Schwegler-Berry, J.F. Scabilloni, V. Castranova, J.M. Antonini, S.S. Leonard, Pulmonary toxicity, distribution, and clearance of intratracheally instilled silicon nanowires in rats, J. Nanomater. 2012 (2012) 1–17.
[207] G. Piret, C.N. Prinz, Could the use of nanowire structures overcome some of the current limitations of brain electrode implants, Nanomedicine 11 (2016) 745–747.
[208] Q. Qing, S.K. Pal, B. Tian, X. Duan, B.P. Timko, T. Cohen-Karni, V.N. Murthy, C.M. Lieber, Nanowire transistor arrays for mapping neural circuits in acute brain slices, Proc. Natl. Acad. Sci. USA 107 (2010) 1882–1887.
[209] J.-H. Lee, A. Zhang, S.S. You, C.M. Lieber, Spontaneous internalization of cell penetrating peptide-modified nanowires into primary neurons, Nano Lett. 16 (2016) 1509–1513.
[210] G. Hong, R.D. Viveros, T.J. Zwang, X. Yang, C.M. Lieber, Tissue-like neural probes for understanding and modulating the brain, Biochemistry 57 (2018) 3995–4004.
[211] A. Zhang, Y. Zhao, S.S. You, C.M. Lieber, Nanowire probes could drive high-resolution brain-machine interfaces, Nano Today 31 (2020) 100821.
[212] B.L. Allen, P.D. Kichambare, A. Star, Carbon nanotube field-effect-transistor-based biosensors, Adv. Mater. 19 (2007) 1439–1451.
[213] N. Gao, T. Gao, X. Yang, X. Dai, W. Zhou, A. Zhang, C.M. Lieber, Specific detection of biomolecules in physiological solutions using graphene transistor biosensors, Proc. Natl. Acad. Sci. USA 113 (2016) 14633–14638.
[214] X. Zhou, J.-Y. Park, S. Huang, J. Liu, P.L. McEuen, Band structure, phonon scattering, and the performance limit of single-walled carbon nanotube transistors, Phys. Rev. Lett. 95 (2005) 146805.
[215] T. Dürkop, S. Getty, E. Cobas, M. Fuhrer, Extraordinary mobility in semiconducting carbon nanotubes, Nano Lett. 4 (2004) 35–39.
[216] W. Fu, L. Jiang, E.P. van Geest, L.M. Lima, G.F. Schneider, Sensing at the surface of graphene field-effect transistors, Adv. Mater. 29 (2017) 1603610.
[217] N. Neophytou, A. Paul, G. Klimeck, Bandstructure effects in silicon nanowire hole transport, IEEE Trans. Nanotechnol. 7 (2008) 710–719.
[218] S. Rosenblatt, Y. Yaish, J. Park, J. Gore, V. Sazonova, P.L. McEuen, High performance electrolyte gated carbon nanotube transistors, Nano Lett. 2 (2002) 869–872.
[219] J. Ye, M.F. Craciun, M. Koshino, S. Russo, S. Inoue, H. Yuan, H. Shimotani, A.F. Morpurgo, Y. Iwasa, Accessing the transport properties of graphene and its

multilayers at high carrier density, Proc. Natl. Acad. Sci. USA 108 (2011) 13002–13006.
[220] A. Kim, C.S. Ah, H.Y. Yu, J.-H. Yang, I.-B. Baek, C.-G. Ahn, C.W. Park, M.S. Jun, S. Lee, Ultrasensitive, label-free, and real-time immunodetection using silicon field-effect transistors, Appl. Phys. Lett. 91 (2007) 103901.
[221] A. Sharma, S. Hong, R. Singh, J. Jang, Single-walled carbon nanotube based transparent immunosensor for detection of a prostate cancer biomarker osteopontin, Anal. Chim. Acta 869 (2015) 68–73.
[222] D.-J. Kim, I.Y. Sohn, J.-H. Jung, O.J. Yoon, N.-E. Lee, J.-S. Park, Reduced graphene oxide field-effect transistor for label-free femtomolar protein detection, Biosens. Bioelectron. 41 (2013) 621–626.

Anqi Zhang is currently a postdoctoral scholar working with Professor Zhenan Bao in the Department of Chemical Engineering and Professor Karl Deisseroth in the Department of Bioengineering at Stanford University. She received her Ph.D. degree under the supervision of Professor Charles M. Lieber in the Department of Chemistry and Chemical Biology at Harvard University in 2020, and her B.S. degree in Materials Chemistry from Fudan University in 2014. Her research interests include flexible and stretchable nano-/micro-bioelectronic tools and their applications in neural interfaces. She has published 17 peer-reviewed papers and the book "Nanowires: Building Blocks for Nanoscience and Nanotechnology".

Jae-Hyun Lee is currently an assistant professor of Nano Biomedical Engineering Graduate Program at Yonsei University, Seoul, Korea. He received his Ph.D. degree of Chemistry at Yonsei University in 2011 and worked as a post-doctoral fellow for Professor Charles M. Lieber in the Department of Chemistry and Chemical Biology at Harvard University. His research interests include nanowire and nanoparticle enabled bioelectronic devices and their applications to control cell functions at molecular level. He has published 40 peer-reviewed papers and is the first recipient of Nanotechnology Young researcher Award by IOP publishing.

Charles M. Lieber is the Joshua and Beth Friedman University Professor at Harvard University. Lieber is an elected member of the National Academy of Sciences, the National Academy of Engineering, and the National Academy of Medicine. Lieber has pioneered the field of nanoscience and emerging nanotechnologies, including ground-breaking advances at the boundary between nanoelectronics and medicine. He has published over 400 articles that have been cited more than 105,000 times.